

Extinction theorem for object scattering in a stratified medium

Purnima Ratilal and Nicholas C. Makris

Massachusetts Institute of Technology, Cambridge, Massachusetts 02139

(Received 20 December 2000; revised 13 June 2001; accepted 10 July 2001)

A simple relation for the rate at which energy is extinguished from the incident wave of a far field *point source* by an obstacle of arbitrary size and shape in a *stratified medium* is derived from wave theory. This relation generalizes the classical extinction theorem, or optical theorem, that was originally derived for *plane wave* scattering in free space and greatly facilitates extinction calculations by eliminating the need to integrate energy flux about the obstacle. The total extinction is shown to be a linear sum of the extinction of each wave guide mode. Each modal extinction involves a sum over all incident modes that are scattered into the extinguished mode and is expressed in terms of the object's plane wave scatter function in the forward azimuth and equivalent plane wave amplitudes of the modes. The only assumptions are that multiple scattering between the object and wave guide boundaries is negligible, and the object lies within a constant sound speed layer. Modal extinction cross sections of an object for the extinction of the individual modes of a wave guide are then defined. Calculations for a shallow water wave guide show that, after correcting for absorption loss in the medium, the modal cross section of an object for mode 1 in a typical ocean wave guide is very nearly equal to its free space cross section. This new extinction theorem may be applied to estimate the cross section of an object submerged in a wave guide from a measurement of its forward scattered field. © 2001 Acoustical Society of America. [DOI: 10.1121/1.1405522]

PACS numbers: 43.30.Ft, 43.30.Bp, 43.30.Gr [DLB]

I. INTRODUCTION

If an object is placed in the path of an incident wave, some of the intercepted power is scattered in all direction and the remainder is absorbed. The total power removed from the incident field as a result of scattering and absorption by the object is called extinction.¹ Van de Hulst has shown, in what has become known alternatively as the *extinction theorem*, *optical theorem*, and *forward scatter theorem*, that the extinction can be derived from the scattered far field in the forward direction. Specifically, the total extinction of a plane wave incident on an object in free space equals the imaginary part of the forward scatter amplitude multiplied by the incident intensity and $4\pi/k^2$ where k is the wave number.²⁻⁴ This remarkably simple relationship reflects the fact that the extinction caused by the obstacle leads to shadow formation via destructive interference between the incident and forward scattered fields. The permanence of the extinction is maintained by the formation of a region of destructive interference that survives as an active *shadow remnant*³ in perpetuity beyond the deep shadow.

The total power scattered by an object can be found by integrating the scattered intensity over a large control surface enclosing the object in the far field. This integration is usually difficult to perform and makes an alternative approach attractive. For nonabsorbing objects, the total power scattered by the object is the extinction.^{5,6} One great advantage of the extinction theorem is that it eliminates the need to integrate the scattered energy flux around the object.

The extinction theorem is typically applied in acoustics to measure the *extinction* cross section of objects.⁷ This equals twice the object's projected area in the high frequency limit, and so provides a useful method for estimating an object's size. The extinction theorem has many diverse appli-

cations in acoustics, such as those given in Refs. 8 and 9. It can also be used as a "burglar alarm" to detect and classify intruding objects that pass between a source and an acoustic receiver array.

In 1985 Guo¹⁰ extended the extinction theorem to scattering by an object located next to an interface between two distinct acoustic half spaces. He found an expression for the extinction of an incident plane wave in terms of the far-field scattered pressures in the specular reflection and transmission directions, determined by Snell's law. In a wave guide, the effect of multimodal propagation ensures that the field incident on the object will arrive from many distinct directions. This, combined with the effect of absorption loss in the waveguide, will modify the extinction and scattering cross sections from their free space values. The free space extinction theorem and the half-space extension of Guo are therefore not applicable in a wave guide.

Here we use wave theory to derive a generalized extinction theorem by developing a relation for the rate at which energy is extinguished from the incident wave of a far field *point source* by an object of arbitrary size and shape in a *stratified medium*. Like its free space analogue, the relation is again remarkably simple. The total extinction is shown to be a linear sum of the extinction of each wave guide mode. Each modal extinction involves a sum over all incident modes that are scattered into the given mode and is expressed in terms of the object's plane wave scatter function in the forward azimuth and equivalent modal plane wave amplitudes. For the multiple incident plane waves in a wave guide, extinction is a function of not only the forward scatter amplitude for each of the incident plane waves but also depends on the scatter function amplitudes coupling each incident plane wave to all other plane waves with distinct direc-

tions that make up the incident field. The final relation greatly facilitates extinction calculations by eliminating the need to integrate energy flux about the object.

Our derivation begins with the time-harmonic scattered field from an object in a wave guide that is derived directly from Green's theorem.^{11,12} The only simplifying assumptions are that multiple scattering between the object and wave guide boundaries is negligible and that the object lies within a constant sound speed layer. The simplicity of the resulting extinction relation in the wave guide follows from the fact that the full extinction is maintained in the region of active interference and that this region extends into the far field where separation of variables can be invoked. Energy fluxes necessary for the derivation can then be calculated in the far field in terms of wave guide modes and the object's plane wave scattering function.^{12,13}

The extinction cross section of an object is defined as the ratio of its extinction to the rate at which energy is incident on unit cross sectional area of the object.¹ The extinction cross section reduces to the scattering cross section for nonabsorbing objects, and is useful in actively classifying targets since, as the ratio of the total extinction to the incident intensity, it depends only upon scattering properties of the target. This definition, however, is ambiguous in a wave guide because both the incident and scattered fields are comprised by superpositions of plane waves. Here scattering and propagation effects are not generally separable since they are convolved together in the extinction. Additionally, the incident intensity is not spatially constant. In spite of these difficulties, we find it convenient to interpret the extinction cross section for an object in a wave guide as the ratio of the extinction to the incident energy flux per unit area in the radial direction at the object's centroid. This definition is sensible when the object is in a constant sound speed layer and in the far field of the source.

Calculations for a shallow water wave guide, which have great relevance to active detection problems in ocean acoustics, show that an object's cross section for the combined extinction of all the modes of the wave guide is highly dependent on measurement geometry, medium stratification, as well as its scattering properties. In addition, the combined cross section fluctuates rapidly with range due to coherent interference between the modes. The presence of absorption in the medium can also significantly modify a measurement of the total scattering cross section. The practical implication of these findings is that experimental measurements of the total scattering cross section of an obstacle in a wave guide may differ greatly from those obtained for the same obstacle in free space and may lead to errors in target classification if the wave guide effects are not properly taken into account.

For an object submerged in a wave guide, we also define modal cross sections of the object for the extinction of the individual modes of the wave guide. The modal cross section of an object for the extinction of mode 1 in a typical ocean wave guide was found to be nearly equal to the free space cross section of the object. A potential application of the extinction theorem in a wave guide is then the estimation of the size of an object submerged in the wave guide from a measurement of the extinction it causes to mode 1. The gen-

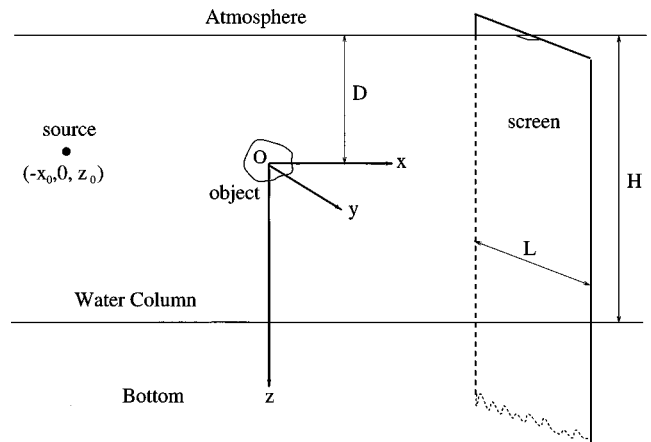


FIG. 1. The geometry of the problem showing an object in a stratified medium composed of a water column of thickness H overlying a bottom. The origin of the coordinate system is at the center of the object and the source is located at $(-x_0, 0, z_0)$. The screen is normal to the x axis with width L and is semi-infinite in the z -direction penetrating into the bottom with an edge at the top of the water column.

eralized extinction theorem can also be used to determine the attenuation due to volume and surface scattering of guided waves propagating through stratified media such as the ocean or the earth's crust.

II. THE GENERALIZED EXTINCTION THEOREM

In this section, we derive the extinction in the incident field of a far field point source due to an obstacle of arbitrary size and shape in a stratified medium. The general approaches for calculating extinction are discussed in Appendix A. Here, we adopt the intuitive approach of Van de Hulst^{1,2,4} which involves integrating the energy flux, or intensity, over a screen placed a distance away from the object sufficiently large to register Fraunhofer diffraction, Eq. (A11). In the absence of the object, the total energy flux across the screen is maximal. In the presence of the object, the total energy flux across the screen is diminished by the shadow remnant. For a sufficiently large screen, the difference between these fluxes is the total extinction.

We focus on the Van de Hulst screen method for calculating extinction because it is of more practical use since it represents the type of measurement that can be made with a standard 2D planar or billboard array. This is discussed further in Sec. V. The other approach for calculating extinction using a control surface that encloses the object in a stratified wave guide is discussed in Appendix D. A control volume measurement would be very difficult to implement since it would require an array that completely encloses the object.

The origin of the coordinate system is placed at the object centroid with z axis vertically downward, and x axis parallel to the boundaries as shown in Fig. 1. The coordinates of the source are defined by $\mathbf{r}_0 = (-x_0, 0, z_0)$. The screen is positioned in forward azimuth on the $y-z$ plane at a horizontal range x from the object center. The width of the screen is L along the y direction and is semi-infinite in the z direction with an edge at the surface of the wave guide. Let $\mathbf{r} = (x, y, z)$ be the coordinates of a point on the screen. Spatial cylindrical (ρ, θ, z) and spherical systems (r, θ, ϕ) are de-

defined by $x = r \sin \theta \cos \phi$, $y = r \sin \theta \sin \phi$, $z = r \cos \theta$ and $\rho = x^2 + y^2$. The horizontal and vertical wave number components for the n th mode are, respectively, $\xi_n = k \sin \alpha_n$ and $\gamma_n = k \cos \alpha_n$ where $k^2 = \xi_n^2 + \gamma_n^2$ and the wave number magnitude k equals the angular frequency ω divided by the sound speed c in the object layer. As discussed in Appendix A to measure the full extinction in the wave guide, we require $L > \sqrt{\lambda x}$, where x is the horizontal range of the screen from the object.

Assuming that the object is far from the source and the screen so that the range from the screen to the source is large, the incident field at location \mathbf{r} on the screen for a source at \mathbf{r}_0 , can be expressed as a sum of normal modes,

$$\Phi_i(\mathbf{r}|\mathbf{r}_0) = \frac{i}{d(z_0)\sqrt{8\pi}} e^{-i\pi/4} \sum_{l=1}^{\infty} u_l(z) u_l(z_0) \frac{e^{i\xi_l|\boldsymbol{\rho}-\boldsymbol{\rho}_0|}}{\sqrt{\xi_l|\boldsymbol{\rho}-\boldsymbol{\rho}_0|}}, \quad (1)$$

where $u_l(z)$ and ξ_l are the l th modal amplitude and horizontal wave number, respectively, and $d(z)$ is the density at depth z .

Using the formulation of Refs. 11 and 12 based on Green's theorem, the scattered field from the object at receiver \mathbf{r} for a source at \mathbf{r}_0 is

$$\begin{aligned} \Phi_s(\mathbf{r}|\mathbf{r}_0) = & \sum_{m=1}^{\infty} \sum_{n=1}^{\infty} \frac{4\pi}{k} \\ & \times [A_m(\mathbf{r})A_n(\mathbf{r}_0)S(\pi - \alpha_m, \phi; \alpha_n, \phi_0 + \pi) \\ & - B_m(\mathbf{r})A_n(\mathbf{r}_0)S(\alpha_m, \phi; \alpha_n, \phi_0 + \pi) \\ & - A_m(\mathbf{r})B_n(\mathbf{r}_0)S(\pi - \alpha_m, \phi; \pi - \alpha_n, \phi_0 + \pi) \\ & + B_m(\mathbf{r})B_n(\mathbf{r}_0)S(\alpha_m, \phi; \pi - \alpha_n, \phi_0 + \pi)], \quad (2) \end{aligned}$$

where

$$\begin{aligned} A_m(\mathbf{r}) = & \frac{i}{d(0)} (8\pi\xi_m\rho)^{-1/2} u_m(z) N_m^- e^{i(\xi_m\rho + \gamma_m D - \pi/4)}, \\ B_m(\mathbf{r}) = & \frac{i}{d(0)} (8\pi\xi_m\rho)^{-1/2} u_m(z) N_m^+ e^{i(\xi_m\rho - \gamma_m D - \pi/4)}, \quad (3) \end{aligned}$$

$$A_n(\mathbf{r}_0) = \frac{i}{d(z_0)} (8\pi\xi_n\rho_0)^{-1/2} u_n(z_0) N_n^- e^{i(\xi_n\rho_0 + \gamma_n D - \pi/4)},$$

$$B_n(\mathbf{r}_0) = \frac{i}{d(z_0)} (8\pi\xi_n\rho_0)^{-1/2} u_n(z_0) N_n^+ e^{i(\xi_n\rho_0 - \gamma_n D - \pi/4)}$$

are the down and up going plane waves in the layer of the object, D is the depth of the object center from the sea surface and $S(\theta, \phi; \theta_i, \phi_i)$ is the object's plane wave scatter function. The definition of the plane wave scatter function here follows that defined in Ref. 12 where the incident plane wave on the object is described in terms of the direction it goes to, so that for forward scatter in free space, $\theta = \theta_i$, $\phi = \phi_i$. The mode functions are normalized according to

$$\delta_{nm} = \int_{-D}^{\infty} \frac{u_m(z) u_n^*(z)}{d(z)} dz, \quad (4)$$

and are decomposable into up- and down-going plane waves in the layer of the object via

$$u_m(z) = N_m^- e^{i\gamma_n(z+D)} - N_m^+ e^{-i\gamma_n(z+D)}. \quad (5)$$

N_n^- and N_n^+ are the amplitudes of the down- and up-going plane waves in this layer.

A number of assumptions have to be satisfied for the above formulation for the scattered field to be valid as noted in Ref. 12. In particular, multiple scattering between the object and wave guide boundaries is negligible, the object lies within a layer of constant sound speed, and the range from the object to source or receiver must be large enough that the scattered field can be approximated as a linear function of the object's plane wave scatter function. The last condition does not limit the generality of the final extinction expression since the full extinction can be registered on sufficiently large screens in the object's far field, but instead simplifies its derivation.

To calculate the extinction using the general formula of Eq. (A11), we first evaluate the integrand for the point \mathbf{r} on the screen. The first term in the integrand of Eq. (A11) using Eqs. (A2), (1), (2), and (3) is

$$\begin{aligned} \mathbf{V}_i^* \Phi_s = & \frac{i}{d(z)d(z_0)d(0)2\omega k} \sum_{l=1}^{\infty} \sum_{m=1}^{\infty} \sum_{n=1}^{\infty} u_l^*(z_0) u_m(z) \left[\frac{\partial}{\partial z} u_l^*(z) \mathbf{i}_z - i \xi_l^* u_l^*(z) \mathbf{i}_x \right] \frac{e^{-i\Re\{\xi_l\} \sqrt{(x_0+x)^2+y^2}}}{\sqrt{\xi_l^*(x_0+x)}} \frac{e^{i\Re\{\xi_m\} \sqrt{x^2+y^2}}}{\sqrt{\xi_m x}} \\ & \times [N_m^- e^{i\Re\{\gamma_m\} D} A_n(\mathbf{r}_0) S(\pi - \alpha_m, \phi; \alpha_n, 0) - N_m^+ e^{-i\Re\{\gamma_m\} D} A_n(\mathbf{r}_0) S(\alpha_m, \phi; \alpha_n, 0) \\ & - N_m^- e^{i\Re\{\gamma_m\} D} B_n(\mathbf{r}_0) S(\pi - \alpha_m, \phi; \pi - \alpha_n, 0) + N_m^+ e^{-i\Re\{\gamma_m\} D} B_n(\mathbf{r}_0) S(\alpha_m, \phi; \pi - \alpha_n, 0)] \\ & \times e^{-\Im\{\xi_l\}(x_0+x)} e^{-\Im\{\xi_m\}x} e^{-\Im\{\gamma_m\}D}. \quad (6) \end{aligned}$$

In the above expression, the terms representing absorption by the wave guide have been factored out explicitly to avoid confusion when conjugating the fields and also to keep track of absorption losses due to the wave guide. The exact expressions for $|\boldsymbol{\rho}-\boldsymbol{\rho}_0| = \sqrt{(x+x_0)^2+y^2}$ and $|\boldsymbol{\rho}| = \sqrt{x^2+y^2}$ were kept in the terms that determine the phase of the integrand

while the approximations $|\boldsymbol{\rho}-\boldsymbol{\rho}_0| \approx (x+x_0)$ and $|\boldsymbol{\rho}| \approx x$ were used in the spreading and absorption loss factors, since $x, x_0 \gg y$ can be satisfied for a screen that measures the full extinction.

Next we integrate Eq. (6) over the area of the screen. With the screen lying parallel to the $y-z$ plane, an area ele-

ment of the screen is $\mathbf{dS}=\mathbf{i}_x dy dz$. We use the orthogonality relation in Eq. (4) between the modes $u_l^*(z)$ and $u_m(z)$ to integrate Eq. (6) over the semi-infinite depth of the screen in the wave guide. This reduces the triple sum over the modes to a double sum:

$$\begin{aligned} \int \int_{S_c} \mathbf{V}_i^* \Phi_s \cdot \mathbf{dS} &= \int_{-L/2}^{L/2} \int_{-D}^{\infty} \mathbf{V}_i^* \Phi_s \cdot \mathbf{i}_x dz dy \\ &= \frac{1}{d(z_0)d(0)2\omega k} \sum_{m=1}^{\infty} \sum_{n=1}^{\infty} \frac{\xi_m^*}{|\xi_m| \sqrt{x(x_0+x)}} u_m^*(z_0) \\ &\quad \times \left\{ \int_{-L/2}^{L/2} [N_m^- e^{i\Re\{\gamma_m\}D} A_n(\mathbf{r}_0) S(\pi - \alpha_m, \phi; \alpha_n, 0) - N_m^+ e^{-i\Re\{\gamma_m\}D} A_n(\mathbf{r}_0) S(\alpha_m, \phi; \alpha_n, 0) \right. \\ &\quad \left. - N_m^- e^{i\Re\{\gamma_m\}D} B_n(\mathbf{r}_0) S(\pi - \alpha_m, \phi; \pi - \alpha_n, 0) + N_m^+ e^{-i\Re\{\gamma_m\}D} B_n(\mathbf{r}_0) S(\alpha_m, \phi; \pi - \alpha_n, 0)] \right. \\ &\quad \left. \times e^{i\Re\{\xi_m\}(\sqrt{x^2+y^2} - \sqrt{(x_0+x)^2+y^2}) dy} \right\} e^{-\Im\{\xi_m\}(x_0+2x)} e^{-\Im\{\gamma_m\}D}. \end{aligned} \quad (7)$$

In the above expression, the scatter function is dependent on y via the azimuth angle $\phi = \tan^{-1}(y/x)$. As discussed in Appendix A, the angular width of the active area on the screen in azimuth is of the order of $\sqrt{\lambda/x}$. We can therefore approximate the scatter function with its value at $\phi=0$ and factor it from the integral above since x is large. We also expand the exponent involving the variable y according to

$$\sqrt{(x_0+x)^2+y^2} \approx x_0+x + \frac{y^2}{2(x_0+x)}, \quad (8)$$

$$\sqrt{x^2+y^2} \approx x + \frac{y^2}{2x}. \quad (9)$$

Applying the result of the following asymptotic integration over the width of the screen,

$$\int_{-L/2}^{L/2} S(\pi - \alpha_m, \phi; \alpha_n, 0) e^{i\Re\{\xi_m\}(\sqrt{x^2+y^2} - \sqrt{(x_0+x)^2+y^2})} dy = e^{-i\Re\{\xi_m\}x_0} S(\pi - \alpha_m, 0; \alpha_n, 0) e^{i\pi/4} \sqrt{\frac{2\pi x(x_0+x)}{\Re\{\xi_m\}x_0}}, \quad (10)$$

to Eq. (7), the integration of the first term in Eq. (A11) over the area of the screen in the wave guide becomes

$$\begin{aligned} \int \int_{S_c} \mathbf{V}_i^* \Phi_s \cdot \mathbf{dS} &= \frac{i}{d^2(z_0)d(0)4\omega k} \frac{1}{x_0} \sum_{m=1}^{\infty} \sum_{n=1}^{\infty} \frac{\xi_m^*}{|\xi_m| \sqrt{\Re\{\xi_m\}\xi_n}} u_m^*(z_0) u_n(z_0) e^{i\Re\{\xi_n - \xi_m\}x_0} \\ &\quad \times [N_m^- N_n^- e^{i\Re\{\gamma_m + \gamma_n\}D} S(\pi - \alpha_m, 0; \alpha_n, 0) - N_m^+ N_n^- e^{i\Re\{-\gamma_m + \gamma_n\}D} S(\alpha_m, 0; \alpha_n, 0) \\ &\quad - N_m^- N_n^+ e^{i\Re\{\gamma_m - \gamma_n\}D} S(\pi - \alpha_m, 0; \pi - \alpha_n, 0) + N_m^+ N_n^+ e^{i\Re\{-\gamma_m - \gamma_n\}D} S(\alpha_m, 0; \pi - \alpha_n, 0)] \\ &\quad \times e^{-\Im\{\xi_m + \xi_n\}x_0} e^{-\Im\{2\xi_m\}x} e^{-\Im\{\gamma_m + \gamma_n\}D}. \end{aligned} \quad (11)$$

Similarly, we can evaluate the second term in Eq. (A11) which gives

$$\begin{aligned} \int \int_{S_c} \mathbf{V}_s^* \Phi_i \cdot \mathbf{dS} &= -\frac{i}{d^2(z_0)d(0)4\omega k} \frac{1}{x_0} \sum_{m=1}^{\infty} \sum_{n=1}^{\infty} \frac{\xi_m^*}{|\xi_m| \sqrt{\Re\{\xi_m\}\xi_n^*}} u_m(z_0) u_n^*(z_0) e^{-i\Re\{\xi_n - \xi_m\}x_0} \\ &\quad \times [N_m^- N_n^* e^{-i\Re\{\gamma_m + \gamma_n\}D} S^*(\pi - \alpha_m, 0; \alpha_n, 0) - N_m^+ N_n^* e^{-i\Re\{-\gamma_m + \gamma_n\}D} S^*(\alpha_m, 0; \alpha_n, 0) \\ &\quad - N_m^- N_n^* e^{-i\Re\{\gamma_m - \gamma_n\}D} S^*(\pi - \alpha_m, 0; \pi - \alpha_n, 0) + N_m^+ N_n^* e^{-i\Re\{-\gamma_m - \gamma_n\}D} S^*(\alpha_m, 0; \pi - \alpha_n, 0)] \\ &\quad \times e^{-\Im\{\xi_m + \xi_n\}x_0} e^{-\Im\{2\xi_m\}x} e^{-\Im\{\gamma_m + \gamma_n\}D}. \end{aligned} \quad (12)$$

When we sum Eqs. (11) and (12), taking only the negative of the real part of the sum following Eq. (A11), we obtain the range dependent extinction $\mathcal{E}(x|\mathbf{r}_0)$ of the incident field in a wave guide due to an object at the origin measured by a screen at distance x from the object with source at \mathbf{r}_0 ,

$$\begin{aligned}
\mathcal{E}(x|\mathbf{r}_0) = & \frac{1}{d^2(z_0)d(0)2\omega k} \frac{1}{x_0} \sum_{m=1}^{\infty} \sum_{n=1}^{\infty} \frac{\sqrt{\Re\{\xi_m\}}}{|\xi_m|} \mathcal{J} \left\{ \frac{1}{\sqrt{\xi_n}} u_m^*(z_0) u_n(z_0) e^{i\Re\{\xi_n - \xi_m\}x_0} \right. \\
& \times [N_m^- N_n^- e^{i\Re\{\gamma_m + \gamma_n\}D} S(\pi - \alpha_m, 0; \alpha_n, 0) - N_m^+ N_n^- e^{i\Re\{-\gamma_m + \gamma_n\}D} S(\alpha_m, 0; \alpha_n, 0) \\
& \left. - N_m^- N_n^+ e^{i\Re\{\gamma_m - \gamma_n\}D} S(\pi - \alpha_m, 0; \pi - \alpha_n, 0) + N_m^+ N_n^+ e^{i\Re\{-\gamma_m - \gamma_n\}D} S(\alpha_m, 0; \pi - \alpha_n, 0) \right\} \\
& \times e^{-\Im\{\xi_m + \xi_n\}x_0} e^{-\Im\{2\xi_m\}x} e^{-\Im\{\gamma_m + \gamma_n\}D}. \tag{13}
\end{aligned}$$

From Eq. (13), we see that the total extinction is a linear sum of the extinction of each wave guide mode. The extinction of mode m involves a sum over all incident modes n that are scattered into that extinguished mode and is expressed in terms of the object's plane wave scatter function in the forward azimuth and equivalent plane wave amplitudes of the modes. The extinction decreases with source-object range x_0 in a wave guide due to geometrical spreading, and with source-object and object-receiver ranges, x_0 and x , due to absorption loss in the medium.

A. Effect of multiple incident plane waves

To understand the implications of Eq. (13), we consider several cases and examine the resulting expression for the extinction in each case.

1. Single mode excited by source

First we consider a source that excites only a single mode p . The incident field on the object and at the screen is determined by this single mode p . The triple sum in Eq. (6) reduces to a single sum over m in this case since both l and n can only take on the integer value p . The orthogonality relation between the modes $u_l^*(z)$ and $u_m(z)$ eliminates the sum over m leaving just a single term where $m=p$ in Eq. (7). Consequently, the expression for the extinction will have only one term corresponding to $m=n=p$, the mode excited by the source,

$$\begin{aligned}
\mathcal{E}(x|\mathbf{r}_0) = & \frac{1}{d^2(z_0)d(0)2\omega k} \frac{1}{x_0} \frac{\sqrt{\Re\{\xi_p\}}}{|\xi_p|} |u_p(z_0)|^2 \mathcal{J} \left\{ \frac{1}{\sqrt{\xi_p}} [(N_p^-)^2 e^{i\Re\{2\gamma_p\}D} S(\pi - \alpha_p, 0; \alpha_p, 0) - N_p^+ N_p^- S(\alpha_p, 0; \alpha_p, 0) \right. \\
& \left. - N_p^- N_p^+ S(\pi - \alpha_p, 0; \pi - \alpha_p, 0) + (N_p^+)^2 e^{i\Re\{-2\gamma_p\}D} S(\alpha_p, 0; \pi - \alpha_p, 0) \right\} e^{-\Im\{2\xi_p\}(x_0+x)} e^{-\Im\{2\gamma_p\}D}. \tag{14}
\end{aligned}$$

Even though the scattered field from the object is composed of multiple modes m , only one of these can interfere destructively with the single incident mode p on the screen and it is precisely the scattered mode that has the same elevation angle as the incident mode.

Mode p is made up of an up-going and a down-going plane wave. Two of the four terms in Eq. (14) arise from the *forward* scatter of the up- and down-going plane waves of mode p , while the remaining two terms arise from the scatter of the incident down-going plane wave of mode p to an upgoing plane wave of the same mode and vice versa. This shows that when we have multiple plane waves incident on the object, the extinction will depend on not only the scatter function in the forward direction but also depend on the scatter function amplitudes coupling each incident plane wave to all other plane waves with distinct directions that make up the incident field.

2. Many modes excited by source

For a general harmonic source that excites many modes, the incident field on the screen is a sum of the contribution from various excited modes. Each of these incident modes on the screen will only interfere destructively in the forward azimuth with the corresponding scattered mode from the ob-

ject with the same elevation angle. The scattering process causes the various incoming incident modes at the object to be coupled to each outgoing scattered mode through the scatter function and this leads to a *double sum* in the expression for the extinction in Eq. (13).

3. Large object-receiver range, x

Next we consider the scenario where the screen is placed at a sufficiently large distance from the object that only the first mode survives for both the incident field on the screen from the source and the scattered field from the object, i.e., $l=m=1$ in Eq. (6). The field incident on the object is still comprised by a sum over the modes n excited by the source since the range of the source from the object is not too large. The expression for the extinction in Eq. (13) then reduces to a single sum over the incident modes n on the object that are scattered into the outgoing mode $m=1$ that survives at the screen.

4. Large source to object range, x_0

If the source is placed at large distances away from the object, the field incident on the object and on the screen will be determined by the single mode $l=n=1$ that survives while the rest of the modes are stripped due to absorption in the wave guide. The extinction in this case has a single term

in Eq. (13) corresponding to $m=n=1$, the mode that survives at the screen. The expression for the extinction is given by Eq. (14) with $p=1$.

These examples illustrate the fact that it is really the interference between the incident field and the scattered field on the screen that determines the extinction. Only scattered field directions that have a fixed phase relationship with the incident field will contribute to the extinction. In the literature, extinction is often stated to be directly proportional to the forward scatter amplitude of a plane wave in free space. For multiple incident plane waves, however, the extinction is not simply a function of the forward scatter amplitude for each incident plane wave but also depends on the scatter function amplitudes coupling each incident plane wave to all other plane waves with distinct directions that make up the incident field. Guo's¹⁰ result for the extinction of a plane wave by an object placed near an interface between two media can also be interpreted in this way.

B. Effect of absorption by the medium

The extinction of the incident field due to an object in the far field of a point source in free space with absorption in the medium is derived in Appendix C. Comparing the expression for extinction in a wave guide, Eq. (13), with that in free space, Eq. (C14) in Appendix C, we see that absorption in the medium lowers the extinction that we would otherwise measure in a lossless medium. In free space, the term due to absorption by the medium is separable from the properties of the object in the formula for the extinction. These terms, however, are in general, convolved in a wave guide with multimodal propagation. The convolution arises because the absorption loss suffered by each mode varies from mode to mode. Furthermore, the modes have varying elevation angles and they are thus scattered differently by the object depending on the elevation angle of the mode. In the wave guide, the absorption loss term can be separated from the term due to the object only if a single mode is incident on the object as seen from Eq. (14), which is the extinction caused by a single mode. One way this arises naturally in a wave guide is when the source to object separation is large enough that only mode 1 survives in the incident field on the object.

III. TOTAL SCATTERED POWER IN THE WAVE GUIDE

The total power scattered by an object in a wave guide can be obtained by integrating the scattered field intensity $\mathbf{V}_s^* \Phi_s$ around a closed control surface enclosing the object, as described in Eq. (A8). We let the control surface be a semi-infinite cylinder of radius R with a cap at the sea surface where $z = -D$. The axis of the cylinder is parallel to the z axis and passes through the object centroid.

The sea surface is a pressure-release surface where the total field vanishes. Since the incident field in the absence of the object is zero at the sea surface, the scattered field has to vanish as well. The scattered energy flux through the cap of the cylinder at $z = -D$ is zero. We need only integrate the scattered intensity over the curved surface of the cylinder to obtain the total scattered power.

From Eq. (2), we see that the scattered field is expressed as a sum of four terms. The scattered intensity at the surface of the cylinder can therefore be expressed as a sum of 16 terms, the first of which is

$$\begin{aligned}
 (\mathbf{V}_s^* \Phi_s)_1 &= \frac{i2\pi}{d(z)d^2(0)\omega k^2} \sum_{m=1}^{\infty} \sum_{n=1}^{\infty} \sum_{p=1}^{\infty} \sum_{q=1}^{\infty} u_p(z) \\
 &\times \left[\frac{\partial}{\partial z} u_m^*(z) \mathbf{i}_z - i \xi_m^* u_m^*(z) \mathbf{i}_p \right] \frac{e^{i\Re\{\xi_p - \xi_m\}R}}{\sqrt{\xi_m^* \xi_p} R} \\
 &\times N_m^- N_p^- e^{i\Re\{\gamma_p - \gamma_m\}D} A_n^*(\mathbf{r}_0) A_q(\mathbf{r}_0) \\
 &\times S^*(\pi - \alpha_m, \phi; \alpha_n, 0) S(\pi - \alpha_p, \phi; \alpha_q, 0) \\
 &\times e^{-\Im\{\xi_m + \xi_p\}R} e^{-\Im\{\gamma_m + \gamma_p\}D}. \tag{15}
 \end{aligned}$$

An area element on the curved surface of the cylinder is given by $d\mathbf{S} = \mathbf{i}_p R d\phi dz$. Making use of Eq. (4), the orthogonality relation between the modes, we integrate Eq. (15) over the semi-infinite depth of the cylinder and the resulting expression is

$$\begin{aligned}
 &\int \int (\mathbf{V}_s^* \Phi_s)_1 \cdot d\mathbf{S} \\
 &= \int_0^{2\pi} \int_{-D}^{\infty} (\mathbf{V}_s^* \Phi_s)_1 \cdot \mathbf{i}_p dz d\phi \\
 &= \frac{2\pi}{d^2(0)\omega k^2} \sum_{m=1}^{\infty} \sum_{n=1}^{\infty} \sum_{q=1}^{\infty} \frac{\xi_m^*}{|\xi_m|} |N_m^-|^2 A_n^*(\mathbf{r}_0) A_q(\mathbf{r}_0) \\
 &\times \int_0^{2\pi} S^*(\pi - \alpha_m, \phi; \alpha_n, 0) S(\pi - \alpha_m, \phi; \alpha_q, 0) d\phi \\
 &\times e^{-2\Im\{\xi_m\}R} e^{-2\Im\{\gamma_m\}D}. \tag{16}
 \end{aligned}$$

The above integral cannot be further evaluated without specifying the scatter function of the object. In general the total scattered power in the wave guide is a complex expression with a triple sum of 16 integrals. The real part of Eq. (16) gives the triple sum of just the first integral.

If there is no absorption by the object, the extinction caused by the object is due entirely to scattering. If the object is in a perfectly reflecting wave guide or a wave guide with small absorption loss, the total scattered power is the extinction. In that case, the complicated expression with triple sum of 16 integrals discussed above reduces to the simple expression of a double sum and no integral of Eq. (13). In a lossy wave guide, if we measure the extinction around a small control surface enclosing the object, the absorption loss inside the control volume is small and the above holds as well. Therefore, the extinction formula eliminates the need to integrate the scattered energy flux about the object in a wave guide when determining the scattered power.

IV. COMBINED AND MODAL EXTINCTION CROSS SECTIONS

The ratio σ_T between the rate of dissipation of energy and the rate at which energy is incident on unit cross sectional area of an obstacle is called the extinction cross sec-

tion of the obstacle.¹ In the wave guide, the intensity of the incident field on the object at the origin from a source at \mathbf{r}_0 is

$$\begin{aligned} \mathbf{I}_i(0|\mathbf{r}_0) &= \Re\{\mathbf{V}_i^*(0|\mathbf{r}_0)\Phi_i(0|\mathbf{r}_0)\} \\ &= \Re\left\{\frac{i}{d^2(z_0)d(0)8\pi\omega x_0}\sum_p\sum_q u_p^*(z_0)\right. \\ &\quad \left.\times\left[\frac{\partial}{\partial z}u_p^*(z)\right]_{z=0}\mathbf{i}_z-i\xi_p^*u_p^*(0)\mathbf{i}_x\right\}u_q(z_0)u_q(0) \end{aligned}$$

$$\times\left.\frac{e^{i\Re\{\xi_q-\xi_p\}x_0}}{\sqrt{\xi_p^*\xi_q}}e^{-\Im\{\xi_p+\xi_q\}x_0}\right\}. \quad (17)$$

In our derivation, the screen is positioned normal to the x axis and it measures the extinction of the energy flux propagating in the x direction. We therefore normalize this extinction by the component of the incident intensity in the x direction to obtain the extinction cross section σ_T of the object in the wave guide,

$$\begin{aligned} \sigma_T(x|\mathbf{r}_0) &= \frac{\mathcal{E}(x|\mathbf{r}_0)}{\mathbf{I}_i(0|\mathbf{r}_0)\cdot\mathbf{i}_x} = \left(\frac{4\pi}{k}\sum_{m=1}^{\infty}\sum_{n=1}^{\infty}\frac{\sqrt{\Re\{\xi_m\}}}{|\xi_m|}\mathcal{J}\left\{\frac{1}{\sqrt{\xi_n}}u_m^*(z_0)u_n(z_0)e^{i\Re\{\xi_n-\xi_m\}x_0}[N_m^-N_n^-e^{i\Re\{\gamma_m+\gamma_n\}D}S(\pi-\alpha_m,0;\alpha_n,0)\right.}\right. \\ &\quad \left.-N_m^+N_n^-e^{i\Re\{-\gamma_m+\gamma_n\}D}S(\alpha_m,0;\alpha_n,0)-N_m^-N_n^+e^{i\Re\{\gamma_m-\gamma_n\}D}S(\pi-\alpha_m,0;\pi-\alpha_n,0)\right. \\ &\quad \left.+N_m^+N_n^+e^{i\Re\{-\gamma_m-\gamma_n\}D}S(\alpha_m,0;\pi-\alpha_n,0)\right\}e^{-\Im\{\xi_m+\xi_n\}x_0}e^{-\Im\{2\xi_m\}x}e^{-\Im\{\gamma_m+\gamma_n\}D}\right) \\ &\quad \times\left(\sum_p\sum_q\Re\{u_p^*(z_0)u_p^*(0)u_q(z_0)u_q(0)\sqrt{\xi_p^*/\xi_q}e^{i\Re\{\xi_q-\xi_p\}x_0}e^{-\Im\{\xi_p+\xi_q\}x_0}\right)^{-1}. \quad (18) \end{aligned}$$

Equation (18) is due to the combined extinction of all the modes of the wave guide by the object and we define it to be the combined extinction cross section. This combined cross section of an object depends on the properties of the object which are convolved with the properties of the wave guide, as well as the source and object locations.

For a source that excites only a single mode p , the incident intensity on the object in the x direction is

$$\mathbf{I}_i(0|\mathbf{r}_0)_p = \frac{i}{d^2(z_0)d(0)8\pi\omega x_0}|u_p(z_0)|^2|u_p(0)|^2\frac{\Re\{\xi_p^*\}}{|\xi_p|}e^{-\Im\{2\xi_p\}x_0}. \quad (19)$$

Dividing the extinction of mode p by the object in Eq. (14) with the intensity of the incident field composed solely of mode p in Eq. (19), we obtain the cross section of the object for the extinction of mode p ,

$$\begin{aligned} \sigma_p(x) &= \frac{4\pi}{k}\frac{1}{\sqrt{\Re\{\xi_p\}}|u_p(0)|^2}\mathcal{J}\left\{\frac{1}{\sqrt{\xi_p}}[(N_p^-)^2e^{i\Re\{2\gamma_p\}D}S(\pi-\alpha_p,0;\alpha_p,0)-N_p^+N_p^-S(\alpha_p,0;\alpha_p,0)\right. \\ &\quad \left.-N_p^-N_p^+S(\pi-\alpha_p,0;\pi-\alpha_p,0)+(N_p^+)^2e^{i\Re\{-2\gamma_p\}D}S(\alpha_p,0;\pi-\alpha_p,0)]\right\}e^{-\Im\{2\xi_p\}x}e^{-\Im\{2\gamma_p\}D}. \quad (20) \end{aligned}$$

We define Eq. (20) as the modal cross section of the object for the extinction of the individual modes of the wave guide. Analogous to plane waves in free space, the modes in a wave guide are the entity that propagate in the wave guide and determine the energy of the acoustic field in the wave guide. It therefore becomes meaningful to quantify the extinction caused by an object of the individual modes of the wave guide and subsequently the cross section of the object as perceived by the individual modes of the wave guide.

V. ESTIMATION OF OBJECT SIZE FROM EXTINCTION THEOREM IN AN OCEAN WAVE GUIDE

The extinction formula can be used to estimate the size of an object by measuring the extinction it causes in an incident beam. For instance, in astronomy, the size of a meteorite is estimated from the extinction it causes in the light reaching a telescope when the meteorite is in interstellar

space between a star and the telescope, so long as the telescope is large enough to measure the entire shadow remnant.⁴

For an object that is large compared to the wavelength, its extinction cross section in free space, according to Babinet's principle, is equal to twice its geometrical projected area.⁴ If we let T_p be the projected area of the object in the direction of an incident plane wave in free space, we obtain

$$\frac{4\pi}{k^2}\mathcal{J}\{S_f\} = 2T_p. \quad (21)$$

The size of the object is therefore directly related to the free space forward scatter function of the object for objects that are large compared to the wavelength. The forward scatter function can be determined from a measurement of the extinction caused by the object.

Extinction measurements usually involve integrating the intensity of the incident and total fields over a sufficiently large screen that registers the full extinction caused by the object. We measure the incident power on the screen in the absence of the object and the total power in the presence of the object. The difference between these two energy fluxes on the screen is the extinction.

An intensity measurement at a single point in space in the forward scatter direction is typically inadequate. This can be seen from Eq. (C3) for free space, and Eq. (6) in the wave guide, where the interference intensity $\mathbf{V}_i^* \Phi_s$ at a point depends very sensitively on the source and receiver positions which cause rapid fluctuation in the phase term. To determine the forward scatter function from a single receiver in the forward direction then requires extremely accurate knowledge of the source, object and receiver locations. In practical measurements, it may also be difficult to precisely locate the point sensor in the forward direction. This is especially true for large objects as they have very narrow forward scatter function peaks. Equation (C14) for the extinction in free space on the other hand has no phase dependence involving the source or screen position. Extinction measurement over a screen is therefore a more robust method for estimating the forward scatter amplitude and hence the size of an object. For measurements in a shallow water wave guide, the screen over which the intensity is integrated can be either a sufficiently large planar array, or a billboard array whose spacing between the sensor elements satisfies the Nyquist criterion for sampling the field in space.

In a wave guide, the extinction caused by an object, Eq. (13), depends not only upon the properties of the object through the scatter function, but also the properties of the wave guide and the measurement geometry. They are, in general, convolved in the expression for the extinction and are separable only when the incident field is composed of a single mode as evident in Eq. (14). This suggests a possible scenario for extinction measurements in a wave guide to extract the scatter function's forward amplitude and subsequently to estimate the size of an object.

For large source to object separation x_0 , the mode that survives in the incident field is mode 1. Mode 1 of any wave guide propagates almost horizontally and we can approximate its elevation angle as $\alpha_1 \approx \pi/2$. In this case, the four scatter function amplitudes in Eq. (14) can be approximated as $S(\pi/2, 0, \pi/2, 0)$ and factored out of the equation for the extinction. Using the fact that for mode 1, $\Re\{\xi_1\} \gg \Im\{\xi_1\}$ we rewrite the extinction for mode 1 as

$$\begin{aligned} \mathcal{E}(x|\mathbf{r}_0) &= \frac{1}{d^2(z_0)d(0)2\omega k} \frac{1}{x_0} \frac{1}{\Re\{\xi_1\}} |u_1(z_0)|^2 \\ &\times \Im\{S(\pi/2, 0; \pi/2, 0) [(N_1^-)^2 e^{i\Re\{2\gamma_1\}D} \\ &- 2N_1^+ N_1^- + (N_1^+)^2 e^{i\Re\{-2\gamma_1\}D}] \} \\ &\times e^{-\Im\{2\xi_1\}(x_0+x)} e^{-\Im\{2\gamma_1\}D}. \end{aligned} \quad (22)$$

In a Pekeris wave guide,^{14,15} with

$$N_1^+ = N_1^- \approx \frac{1}{i} \sqrt{\frac{d(0)}{2H}}, \quad (23)$$

using Eq. (5), we see that

$$\begin{aligned} |u_1(0)|^2 &= [(N_1^-)^2 e^{i\Re\{2\gamma_1\}D} - 2N_1^+ N_1^- \\ &+ (N_1^+)^2 e^{i\Re\{-2\gamma_1\}D}] e^{-\Im\{2\gamma_1\}D}. \end{aligned} \quad (24)$$

The extinction formula for mode 1 therefore leads to

$$\begin{aligned} \mathcal{E}(x|\mathbf{r}_0) &= \frac{1}{d^2(z_0)d(0)2\omega k} \frac{1}{x_0} \frac{1}{\Re\{\xi_1\}} |u_1(z_0)|^2 |u_1(0)|^2 \\ &\times \Im\{S(\pi/2, 0; \pi/2, 0)\} e^{-\Im\{2\xi_1\}(x_0+x)}. \end{aligned} \quad (25)$$

Equation (20) for the modal cross section of the object for mode 1 in the Pekeris wave guide, simplifies to

$$\sigma_1(x) = \frac{4\pi}{k} \frac{1}{\Re\{\xi_1\}} \Im\{S(\pi/2, 0; \pi/2, 0)\} e^{-2\Im\{\xi_1\}x}. \quad (26)$$

Since mode 1 propagates close to the horizontal, $\Re\{\xi_1\} \approx k$. The cross section of an object for the extinction of mode 1 in a Pekeris wave guide, Eq. (26), is almost identical to the cross section of the object for the extinction of plane waves in free space, Eq. (C16).

In Eqs. (25) and (26) the properties of the target are separated from the wave guide and geometric parameters. If we can measure the extinction of mode 1 caused by the object in the wave guide, we can estimate the free space forward scatter amplitude of the object and subsequently, the size of the object. A knowledge of the wave guide properties, and location of source, object and screen is necessary to correct for the spreading and absorption loss in the wave guide, as well as the amplitude of mode 1 at the source and object depths. Experimentally, we can estimate the source to object range x_0 from the arrival of the back scattered field from the object using a sensor that is co-located with the source.

As discussed in Eq. (21), the object size is related to the forward scatter function amplitude. The extinction of the higher order modes of the wave guide, apart from mode 1, depend on the scatter function amplitude in other directions in addition to the forward. It is therefore much more difficult to extract information about the size of the object from modes higher than mode 1 unless the object is compact as will be discussed in Sec. (VIE). For objects that are buried in sediments that are faster than water, mode 1 excited by a source in the water column does not penetrate into the bottom due to total internal reflection. The above method will therefore not be useful in estimating the size of objects buried in fast bottoms.

VI. ILLUSTRATIVE EXAMPLES

In all the illustrative examples, a water column of 100 m depth is used to simulate a typical continental shelf environment. The sound speed structure of the water column is isovelocity with constant sound speed of 1500 m/s, density of 1 g/cm³ and attenuation of 6.0×10^{-5} dB/λ. The seabed is either perfectly reflecting or comprised of sand or silt half spaces. The density, sound speed and attenuation are taken to be 1.9 g/cm³, 1700 m/s, and 0.8 dB/λ for sand, 1.4 g/cm³, 1520 m/s, and 0.3 dB/λ for silt. Calculations are made of the combined and modal extinction, incident intensity on the ob-

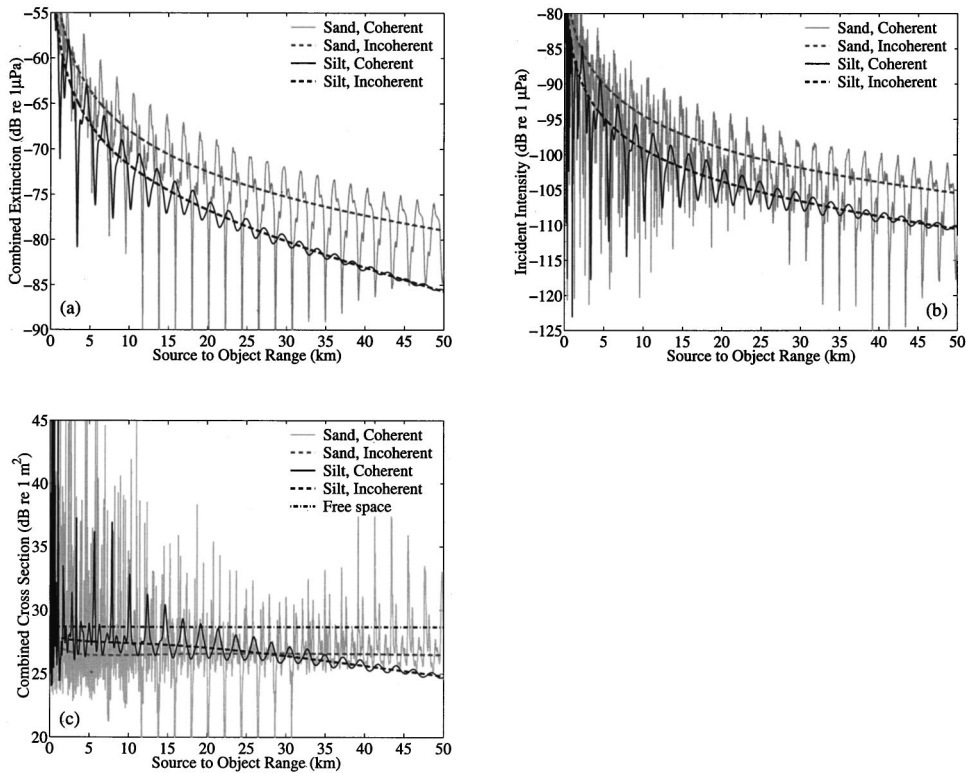


FIG. 2. (a) The combined extinction Eq. (13) of all the modes, caused by a pressure release sphere of radius 10 m centered at 50 m depth, in a Pekeris wave guide composed of 100 m water with either sand or silt half space is plotted as a function of x_0 , its range from a point source of frequency 300 Hz also placed at the same depth in the wave guide. The separation of the screen from the object is the same as that of the source from the object at each source to object range, $x = x_0$. (b) The incident intensity on the sphere Eq. (17). (c) The combined cross section of the sphere Eq. (18). Both the coherent and incoherent approximation of the quantities are plotted in each subfigure.

ject, and, the combined and modal cross sections in various wave guides for different objects as a function of source, object and screen locations. The object size and frequency is also varied. Except for Sec. VIE, the frequency used in all other examples is 300 Hz.

A. Combined extinction cross section in different wave guides

First, we examine how the combined extinction of all the modes, caused by a pressure-release sphere of radius 10 m, in a Pekeris wave guide with either sand or silt bottom half space varies as a function of source to object range at a source frequency of 300 Hz. The source and sphere centers are located at $D = 50$ m in the middle of the water column. The combined extinction measured by the screen Eq. (13), the incident intensity on per unit area of the sphere Eq. (17), and the combined cross section of the sphere Eq. (18) in the wave guides are plotted as a function of source to object separation x_0 in Figs. 2(a)–(c), respectively. At each x_0 , the separation of the screen from the object is the same as that of the source from the object, i.e., $x = x_0$. The combined extinction is calculated using Eq. (13) with the scatter function for the sphere given by Eqs. (8) and (9) of Ref. 13 with $f(n)$ replaced by $(-1)^n f(n)$ to convert from Ingenito’s definition to the standard one described in Ref. 12.

The combined extinction and incident intensity fluctuate with range due to the coherent interference between the modes. The resulting combined cross section of the sphere also fluctuates with range. The incident intensity and extinction are larger in the wave guide with sand bottom. The fluctuations in the fields are also greater in the sand bottom wave guide as compared to the silt bottom wave guide. The difference arise primarily because the number of trapped

modes is larger for the sand half space due to the higher critical angle of 28.1° for the water to sand interface as compared with the 9.3° of water to silt leading to larger fields and fluctuations in the wave guide with sand bottom. For a screen placed at a fixed range from the object, it is the coherent extinction and cross section that we measure experimentally. From Fig. 2(c), we see that the coherent combined cross section of the object varies rapidly with range in the wave guide. Consequently, it is difficult to extract information about the size of the object from a measurement of its combined extinction of all the wave guide modes.

We find it useful to approximate the combined extinction measured by the screen and the incident intensity on the sphere as a single incoherent sum over the modes which provides an average trend to the curves as a function of range. Taking the ratio of the incoherent combined extinction and incident intensity, we obtain the incoherent combined cross section. The combined extinction, incident intensity and combined cross section of the sphere calculated incoherently, using Eqs (13), (17), and (18), respectively, by replacing the double sum with a single sum over the modes are plotted in Figs. 2(a)–(c). From the incoherent plots, we see that the extinction and the incident intensity decay with range due to geometrical spreading and absorption loss in a real wave guide.

In a perfectly reflecting wave guide, there is no absorption in the wave guide. Consequently, an incoherent approximation for σ_T is independent of range as can be seen from Eq. (18). The decay in the extinction due to spreading loss is compensated by spreading loss in the flux incident on the object which keeps the cross section a constant. In this case, the extinction measured by the screen is due entirely to the

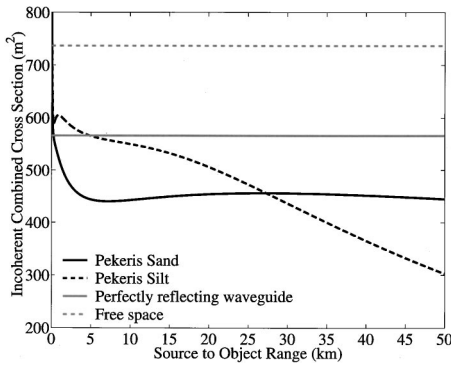


FIG. 3. Incoherent combined cross section of a 10 m radius pressure release sphere at 300 Hz source frequency in a Pekeris wave guide with sand bottom half space, Pekeris wave guide with silt bottom half space, perfectly reflecting wave guide, and free space as a function of source to object range x_0 . For this plot, $x = x_0$. In the wave guides, the source and sphere center are located at 50 m water depth. The incoherent combined cross section is calculated using Eq. (18) by replacing the double sum over the modes with a single sum.

object. Figure 3 shows σ_T , calculated incoherently, plotted for a pressure-release sphere of radius 10 m in a perfectly reflecting wave guide as a function of x_0 . In this figure $x = x_0$. The incoherent combined cross section of the object in free space with no absorption and in the Pekeris wave guide examples considered so far are also plotted for comparison. Figure 3 shows that this incoherent combined cross section for the extinction of all the wave guide modes differs significantly from the free space cross section of the object. So, it is difficult to obtain an estimate of the size of an object from an incoherent as well as a coherent measurement of its combined cross section.

B. Modal cross section in different wave guides

In this section, we will investigate how the modal extinction cross section of the 10 m pressure release sphere varies for the individual modes in various wave guides at 300 Hz. Figures 4(a) and (b) show the amplitudes of the modes at the source depth of 50 m in the Pekeris wave guide with sand and silt bottom, respectively. Only the propagating modes are plotted because these are the modes that compose the incident field on the object in the far field. These are the mode amplitudes at the object depth because the target is also at 50 m depth. The amplitude of the modes in the perfectly reflecting wave guide are plotted in Fig. 4(c). Only the even number modes are excited by the source at 50 m depth and they have the same amplitude.

The extinction of each individual mode in the Pekeris wave guide with sand bottom caused by the sphere and calculated using Eq. (14) are plotted in Figs. 5(a) and (b) at the source to object range of 1 km and 25 km, respectively. The screen is placed the same distance away from the object as the source in each case. The modal extinctions in the Pekeris wave guide with silt bottom at 1 km and 25 km are plotted in Figs. 5(c) and (d), respectively. Comparing Fig. 5 with Fig. 4, we see a dependence of the extinction of each mode on its amplitude at the object depth, with the more energetic modes being extinguished the most. The extinction of the modes vary with range due to spreading and absorption loss suffered by the modes. Absorption loss suffered by each mode as a result of absorption in a real wave guide is more severe for the high order modes due to their steeper elevation angles. The higher order modes are gradually stripped with increasing range and at sufficiently long ranges, the extinction caused by the object is very much limited to the extinc-

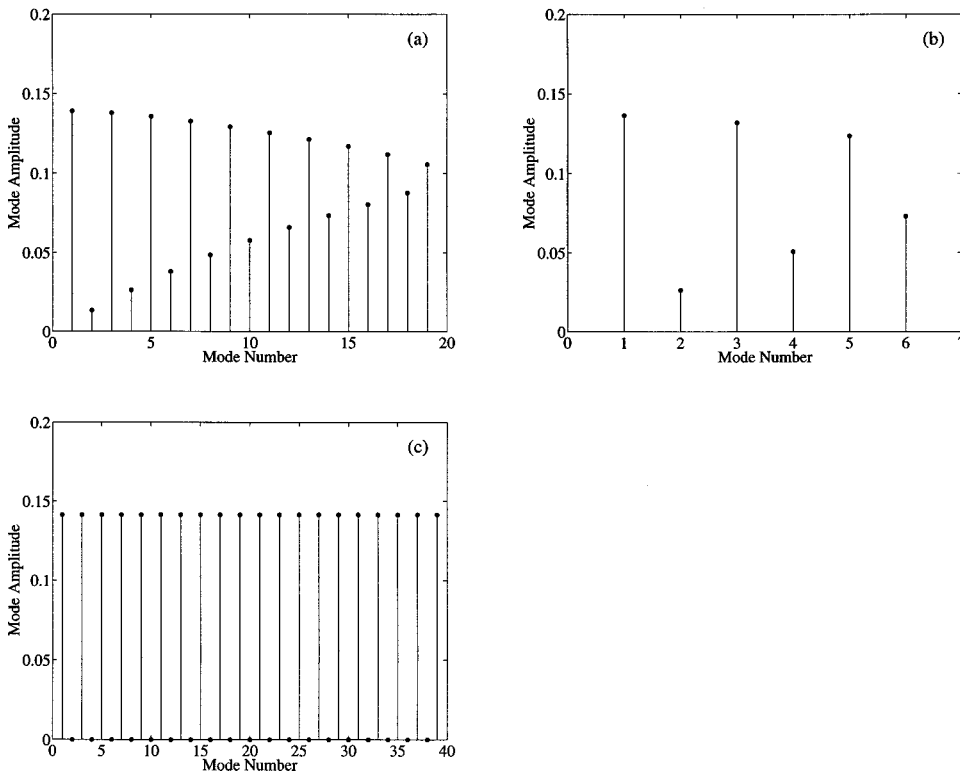


FIG. 4. Modal amplitude at the source and target depth of 50 m in (a) Pekeris wave guide with sand half space, (b) Pekeris wave guide with silt half space, and (c) perfectly reflecting wave guide for a frequency of 300 Hz.

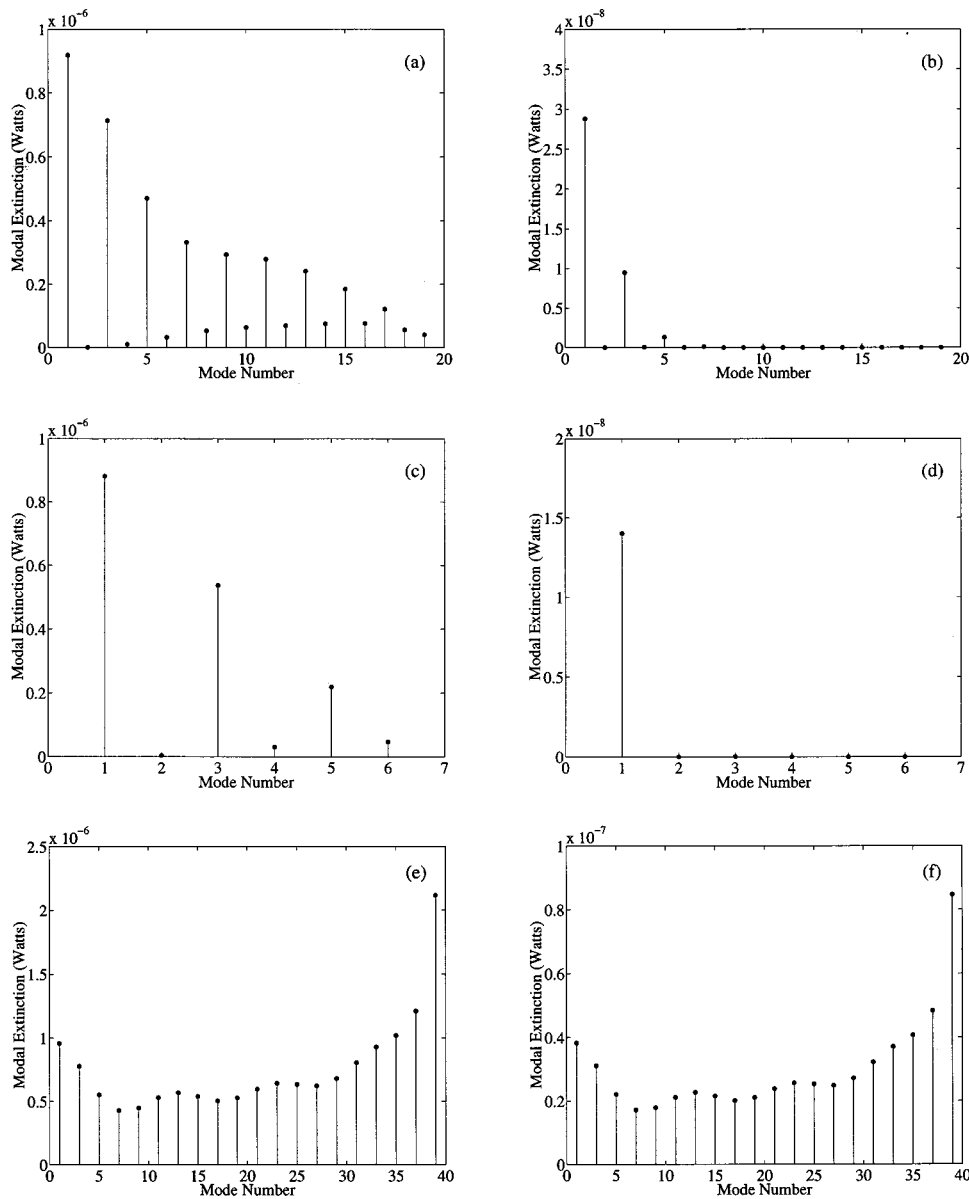


FIG. 5. Extinction of the individual modes Eq. (14) of the wave guide by the 10 m radius pressure release sphere at 50 m water depth with the source separated from the sphere by (a) 1 km range in a Pekeris sand half space wave guide, (b) 25 km range in a Pekeris sand half space wave guide, (c) 1 km range in a Pekeris silt half space wave guide, (d) 25 km range in a Pekeris silt half space wave guide, and (e) 1 km range in a perfectly reflecting wave guide, (f) 25 km range in a perfectly reflecting wave guide. The source depth is also 50 m and the source frequency is 300 Hz. The screen measuring the extinction is separated the same distance from the object as the source in each case.

tion of the first few propagating modes. For the perfectly reflecting wave guide in Figs. 5(e) and (f) at 1 km and 25 km, respectively, there is no absorption loss, so the extinction for each mode decays only with source to object range x_0 . There is no mode stripping effect in a perfectly reflecting wave guide and the relative magnitude of the extinction across the modes remains the same, independent of range.

Figures 6(a)–(c) show the modal cross sections of the sphere, calculated using Eq. (20), for the extinction of the individual modes in the Pekeris sand, silt and perfectly reflecting wave guides, respectively. We set $x = 0$ in Eq. (20) to obtain the modal cross section of the object corrected for absorption in the wave guide. In each of the wave guides illustrated in Fig. 6 we see that the modal cross section of the sphere for the extinction of mode 1 is very close to its cross section for the extinction of a plane wave in free space. For the higher order modes, the modal cross section of the object can be much larger or smaller than its free space value depending on the wave guide. We can calculate the forward scatter function amplitude of the object from a measurement

of the extinction of mode 1 as discussed in Sec. V which allows us to estimate the size of the object.

C. Dependence of modal cross section on object depth

The modal cross section of an object depends on the depth of the object in the wave guide. We investigate how the modal cross section of the 10 m pressure release sphere varies when we lower its depth by half a wavelength distance to 52.5 m in the Pekeris silt, sand, and perfectly reflecting wave guides. We also lower the source depth to 52.5 m so that all the modes in the perfectly reflecting wave guide are excited by the source. The source frequency is 300 Hz.

Figure 7 shows the incoherent combined cross section of the sphere in the three wave guides. In the perfectly reflecting wave guide, the incoherent combined cross section of the sphere is now larger than its free space value. Figures 8(a)–(c) show the modal amplitudes in the three wave guides and

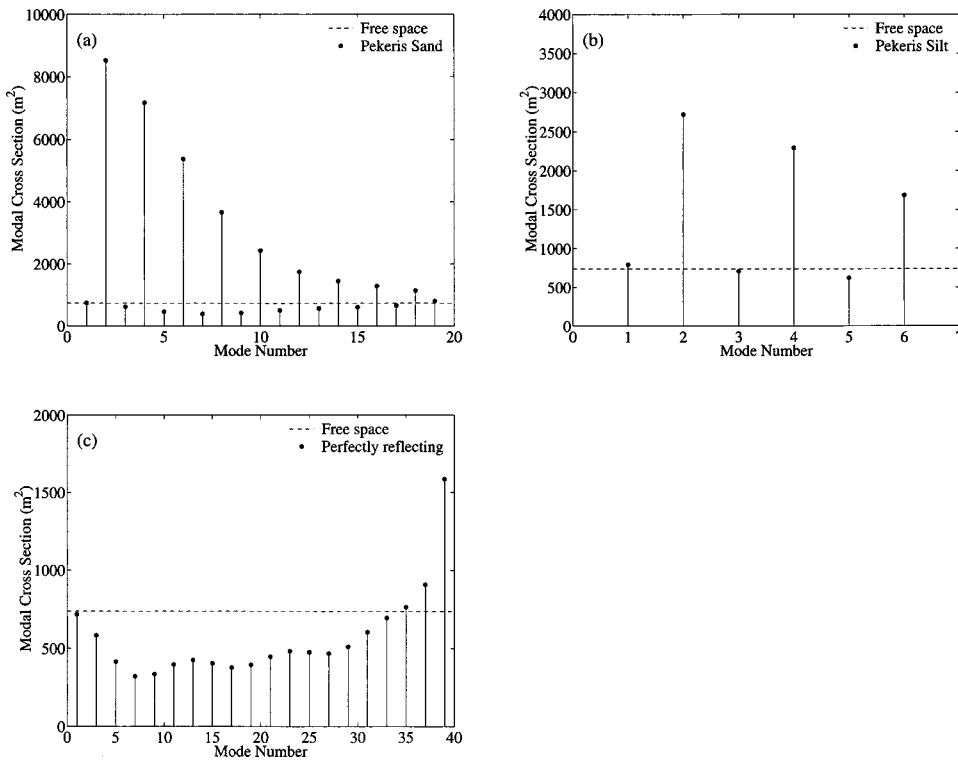


FIG. 6. Modal cross section Eq. (20) at 300 Hz of the 10 m radius pressure release sphere at 50 m water depth for the extinction of the individual modes in a (a) Pekeris sand half space wave guide, (b) Pekeris silt half space wave guide, and (c) perfectly reflecting wave guide. We set $x=0$ in Eq. (20) to remove the effect of absorption by the wave guide. The modal cross section of the sphere for mode 1 in each wave guide is almost equal to its free space cross section.

Figs. 9(a)–(c) show the modal cross sections, Eq. (20). In the perfectly reflecting wave guide Fig. 9(c), all modes that exist in the wave guide are scattered by the object to form the scattered field when it is at the shallower depth of 52.5 m, unlike in the previous example of Fig. 6 where it was at 50 m depth and only the excited odd number modes were scattered by the object. Comparing Fig. 9 with Fig. 6, we see that the modal cross section of most of the modes vary with object depth. For mode 1, however, in all the three wave guides, the modal cross section of the object remains close to its free space value.

D. Modal cross section for various object types

The cross section of the 10 m pressure release sphere is compared to that of a rigid or hard disk of radius 10 m in the

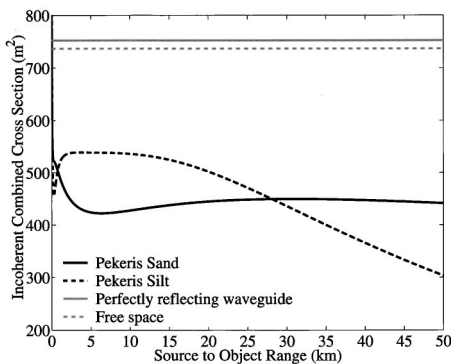


FIG. 7. Incoherent combined cross section of a 10 m radius pressure release sphere at 300 Hz source frequency in a Pekeris wave guide with sand bottom half space, Pekeris wave guide with silt bottom half space, perfectly reflecting wave guide, and free space as a function of source to object range x_0 . For this plot, $x=x_0$. In the wave guides, the source and sphere center are located at 52.5 m water depth. The incoherent combined cross section is calculated using Eq. (18) by replacing the double sum over the modes with a single sum.

wave guide. In free space, with the plane of the disk aligned normal to the direction of propagation of the incident waves, it is well known that its plane wave extinction cross section is equal to twice its projected area, which is 628.3 m^2 in this example. The cross section of a sphere in free space depends on the circumference of the sphere relative to the wavelength of the incident waves, i.e., $ka=2\pi a/\lambda$ where a is the radius of the sphere. The dependence of the extinction cross section of a pressure release or hard sphere on ka , in free space is plotted in Ref. 16. For a large pressure release sphere, high ka , the extinction cross section is roughly twice the projected area which is the same for both the sphere and the disk. For a compact pressure release sphere, small ka , the cross section of the sphere begins to exceed twice its projected area. For the present example, at 300 Hz source frequency, $ka=12.6$ and the extinction cross section of the sphere in free space is 736.7 m^2 .

The incoherent combined cross section of the 10 m hard disk in the three different wave guides is plotted in Fig. 10. In free space, the cross section of the sphere at 300 Hz is only a little larger than that of the disk of the same radius. Comparing Figs. 3 and 10, we see that in the perfectly reflecting wave guide, the incoherent combined cross section of the sphere is much larger than that of the disk. The elevation angle of each mode of the wave guide increases with the mode number. Since the disk is aligned with its plane parallel to the $y-z$ plane, the projected area of the disk perceived by each mode decreases as the elevation angle of the mode increases. For the sphere, however, each mode sees the same projected area, regardless of the elevation angle of the mode. Therefore the combined extinction of the modes by the sphere is much larger than by the disk. In the real wave guide, absorption by the wave guide alters the amplitude of each mode with the higher order modes

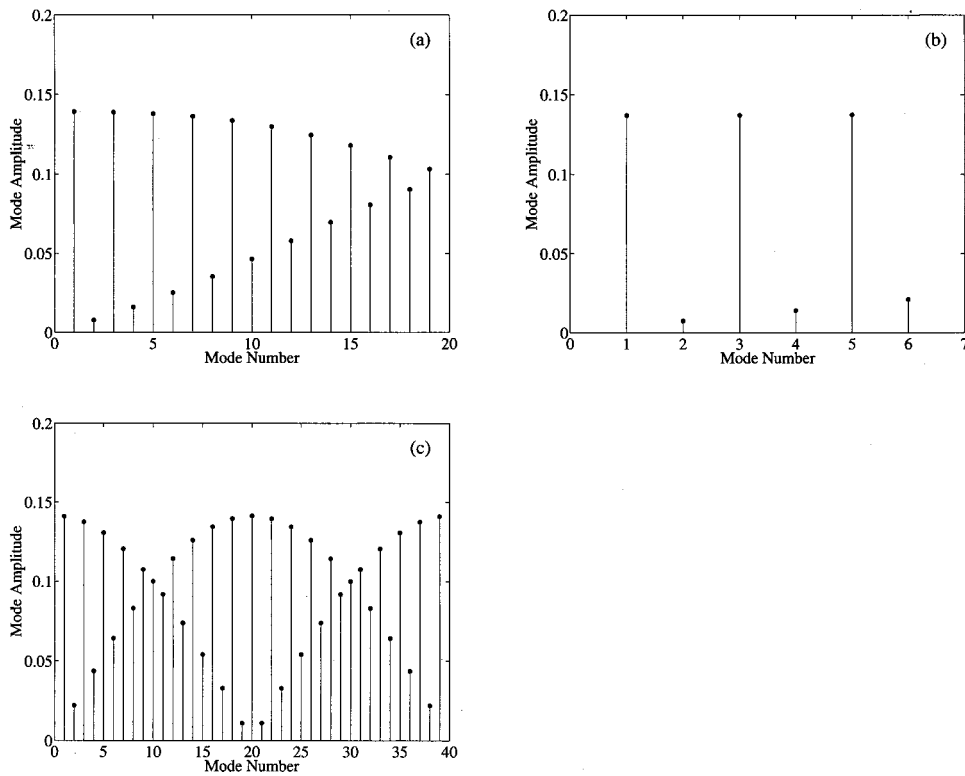


FIG. 8. Modal amplitude at the object depth of 52.5 m in (a) Pekeris wave guide with sand half space, (b) Pekeris wave guide with silt half space, and (c) perfectly reflecting wave guide for a frequency of 300 Hz.

suffering greater absorption losses than the lower order modes. The higher order modes are less important in determining the combined extinction in the real wave guide. Consequently, in a real wave guide, the incoherent combined cross section of the sphere is only slightly larger than that of the disk.

The modal cross section Eq. (20) of the disk for each mode of the Pekeris sand, silt, and the perfectly reflecting

wave guide is plotted in Figs. 11(a)–(c), respectively. From Fig. 11, we see once again that the modal cross section of the object for the extinction of mode 1 is almost equal to its free space cross section. In the present example, the cross section of the disk is equal to twice its projected area. This example further illustrates that we can obtain a measure of the size of an object from the extinction of mode 1 in a wave guide.

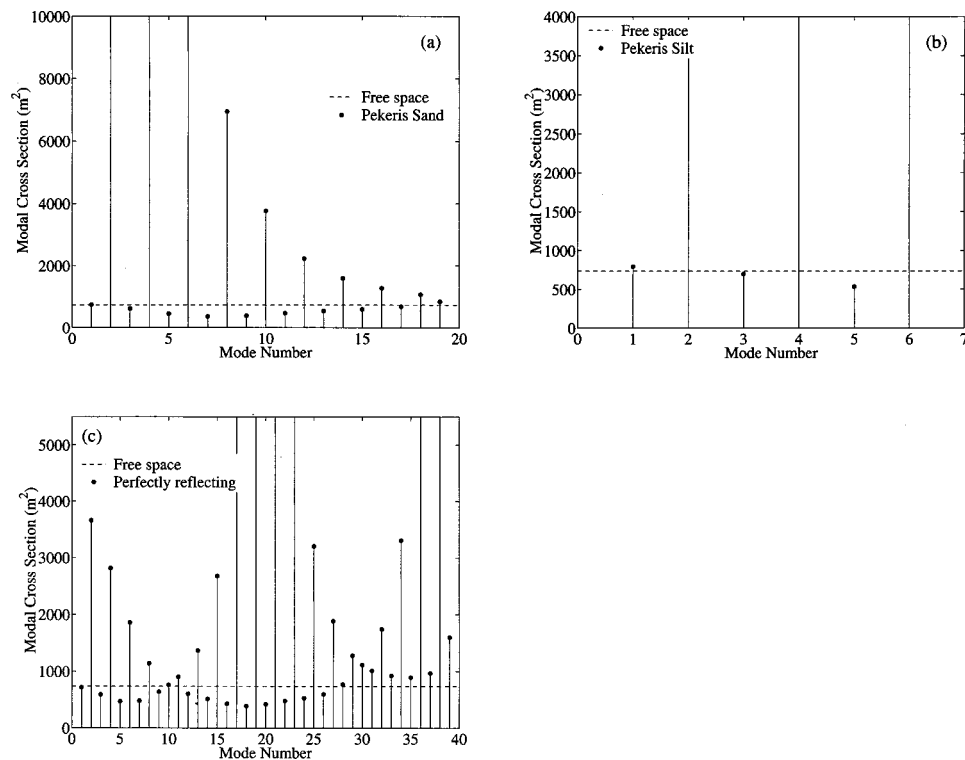


FIG. 9. Modal cross section Eq. (20) at 300 Hz of the 10 m radius pressure release sphere at 52.5 m water depth for the extinction of the individual modes in (a) Pekeris sand half space wave guide, (b) Pekeris silt half space wave guide, and (c) perfectly reflecting wave guide. We set $x=0$ in Eq. (20) to remove the effect of absorption by the wave guide. The modal cross section of the sphere for mode 1 in each wave guide is almost equal to its free space cross section.

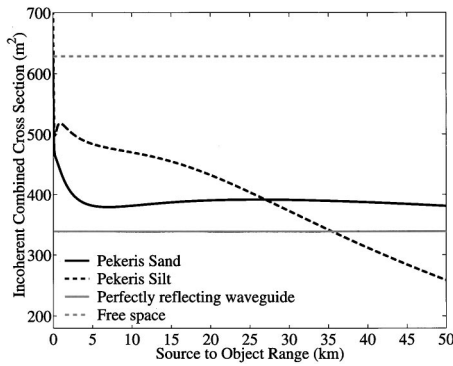


FIG. 10. Incoherent combined cross section of a hard disk of radius 10 m at 300 Hz source frequency in a Pekeris wave guide with sand bottom half space, Pekeris wave guide with silt bottom half space, perfectly reflecting wave guide, and free space as a function of source to object range x_0 . For this plot, $x = x_0$. In the wave guides, the source and disk center are located at 50 m water depth with the disk aligned in the $y-z$ plane. The incoherent combined cross section is calculated using Eq. (18) by replacing the double sum over the modes with a single sum.

E. Dependence of modal cross section on object size and frequency

Here we investigate how the modal cross section Eq. (20) of a pressure release sphere at 50 m water depth compares with its free space cross section when we vary the size of the sphere and the frequency of the incoming waves. Figures 12(a)–(d) show the result in a Pekeris sand wave guide, plotted as a function of ka . The corresponding result in the Pekeris silt and perfectly reflecting wave guides are plotted in Figs. 13 and 14, respectively.

For a large sphere with the high ka of 62.8, we see from Figs. 12–14(d) that the modal cross section of the sphere for the high order modes fluctuates and departs drastically from the free space cross section for most of the modes. The

modal cross section for mode 1, however, remains nearly equal to the free space cross section of the large sphere in each wave guide. For the compact sphere with the small ka of 0.1 on the other hand, Figs. 12–14(a), the modal cross section of most of the modes are fairly close to the free space cross section of the object.

Figures 15(a)–(d) show the scatter function amplitude plotted as a function of elevation angle of the modes at various ka . Compact objects scatter like point targets and they have an omnidirectional scatter function S_0 . In Eq. (20), we see that the modal cross section depends on not only the forward scatter amplitude, but also the scatter function amplitude in nonforward directions. For a compact object, since the scatter function amplitude is a constant, independent of azimuth or elevation angles, we can factor it out in Eq. (20). Furthermore, in a perfectly reflecting wave guide, since^{14,15}

$$N_p^+ = N_p^- = \frac{1}{i} \sqrt{\frac{d(0)}{2H}}, \quad (27)$$

N_p can be factored out of the equation as well. Consequently, for a compact object in the perfectly reflecting wave guide, Eq. (20) for the modal cross section reduces to

$$\sigma_p(x) = \frac{4\pi}{k} \frac{1}{\Re\{\xi_p\}} \mathcal{T}\{S_0\} e^{-2\Im\{\xi_p\}x} \quad (28)$$

which resembles the expression for the free space cross section of the object in Eq. (C16). The modal cross section of the compact object in the wave guide will, however, be slightly larger than the free space cross section because of the dependence on the horizontal wave number of the mode ξ_p in the denominator of Eq. (28) instead of k as in Eq. (C16) for free space. The real part of the horizontal wave number decreases as the mode number increases. We see a gradual

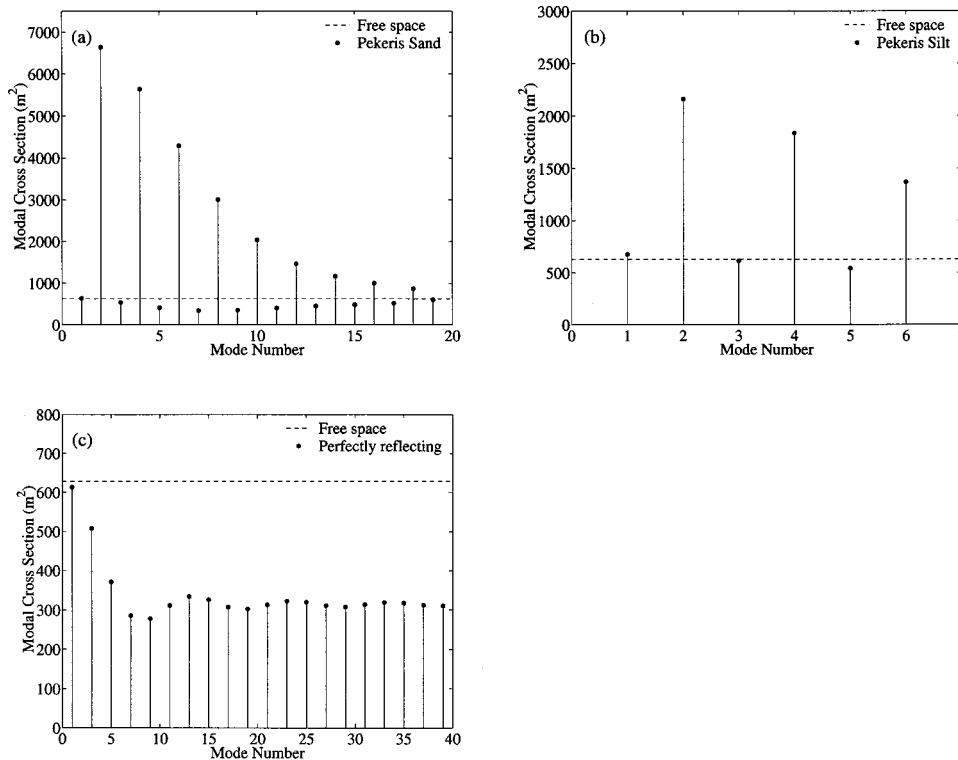


FIG. 11. Modal cross section Eq. (20) at 300 Hz of the 10 m radius hard disk at 50 m water depth for the extinction of the individual modes in a (a) Pekeris sand half space wave guide, (b) Pekeris silt half space wave guide, and (c) perfectly reflecting wave guide. We set $x=0$ in Eq. (20) to remove the effect of absorption by the wave guide. The modal cross section of the disk for mode 1 in each wave guide is almost equal to its free space cross section.

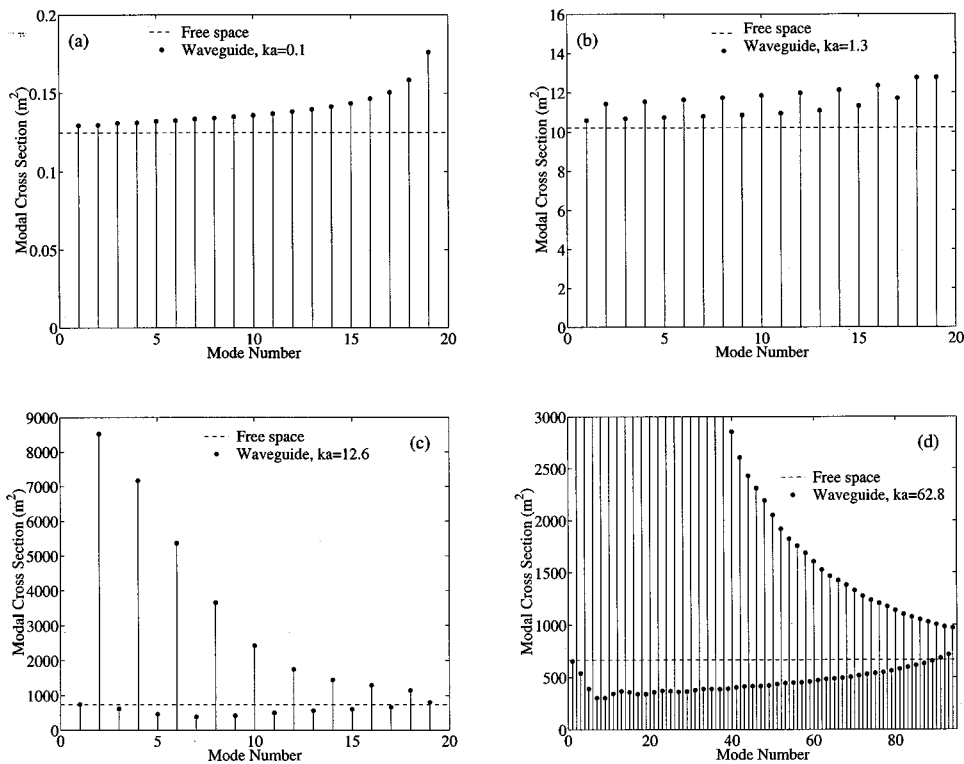


FIG. 12. Modal cross section Eq. (20) of a pressure release sphere at 50 m water depth for the extinction of the individual modes in a Pekeris sand half space wave guide with (a) sphere radius 0.1 m, 300 Hz source frequency, $ka=0.1$, (b) sphere radius 1 m, 300 Hz source frequency, $ka=1.3$, (c) sphere radius 10 m, 300 Hz source frequency, $ka=12.6$, and (d) sphere radius 10 m, 1500 Hz source frequency, $ka=62.8$. We set $x=0$ in Eq. (20) to remove the effect of absorption by the wave guide. Only the propagating modes are illustrated in each plot. The modal cross section of the sphere for mode 1 in each case is almost equal to its free space cross section.

increase in the modal cross section in Fig. 14(a) with increase in mode number for the compact sphere in the perfectly reflecting wave guide.

In a real wave guide, N_p is usually complex. For the lower order modes, N_p has a large imaginary component and we can still factor it out as we did for the perfectly reflecting wave guide. We also observe a trend of increase in modal cross section with mode number for the compact sphere in the examples of Figs. 12–13(a). This implies that for a com-

compact object in a wave guide, as well as mode 1, we can also use the higher order modes to extract its omnidirectional scatter function amplitude from modal extinction measurements. Once the scatter function amplitude of a compact object is known, its size can be estimated.

VII. SUMMARY AND DISCUSSION

A generalized extinction theorem for the rate at which energy is extinguished from the incident wave of a far field

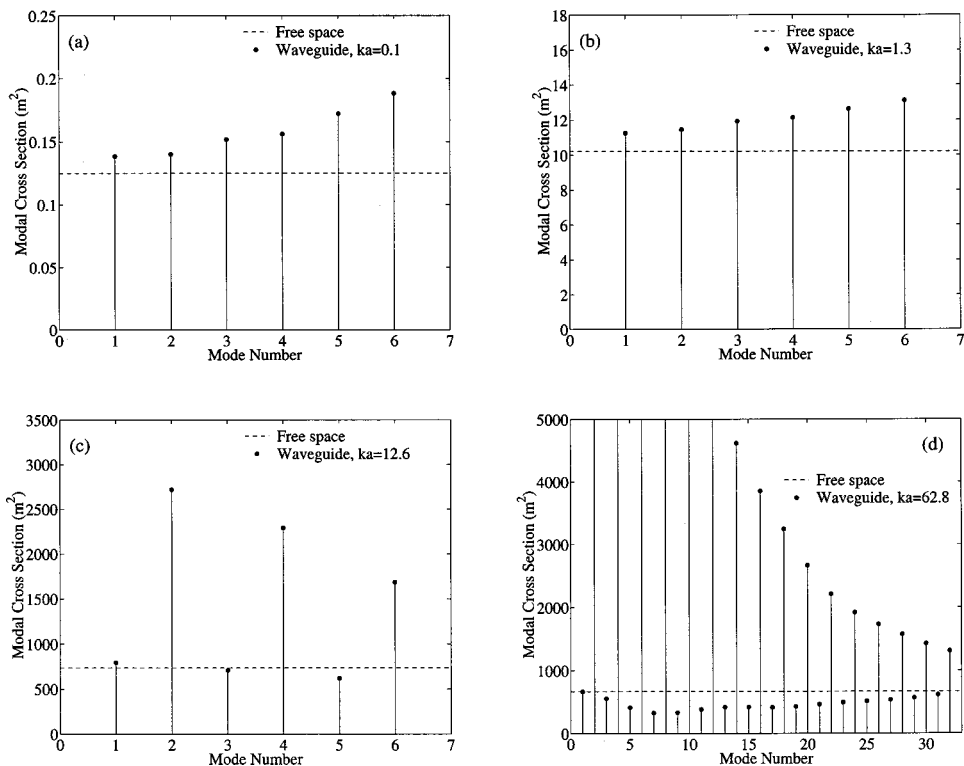


FIG. 13. Modal cross section Eq. (20) of a pressure release sphere at 50 m water depth for the extinction of the individual modes in a Pekeris silt half space wave guide with (a) sphere radius 0.1 m, 300 Hz source frequency, $ka=0.1$, (b) sphere radius 1 m, 300 Hz source frequency, $ka=1.3$, (c) sphere radius 10 m, 300 Hz source frequency, $ka=12.6$, and (d) sphere radius 10 m, 1500 Hz source frequency, $ka=62.8$. We set $x=0$ in Eq. (20) to remove the effect of absorption by the wave guide. Only the propagating modes are illustrated in each plot. The modal cross section of the sphere for mode 1 in each case is almost equal to its free space cross section.

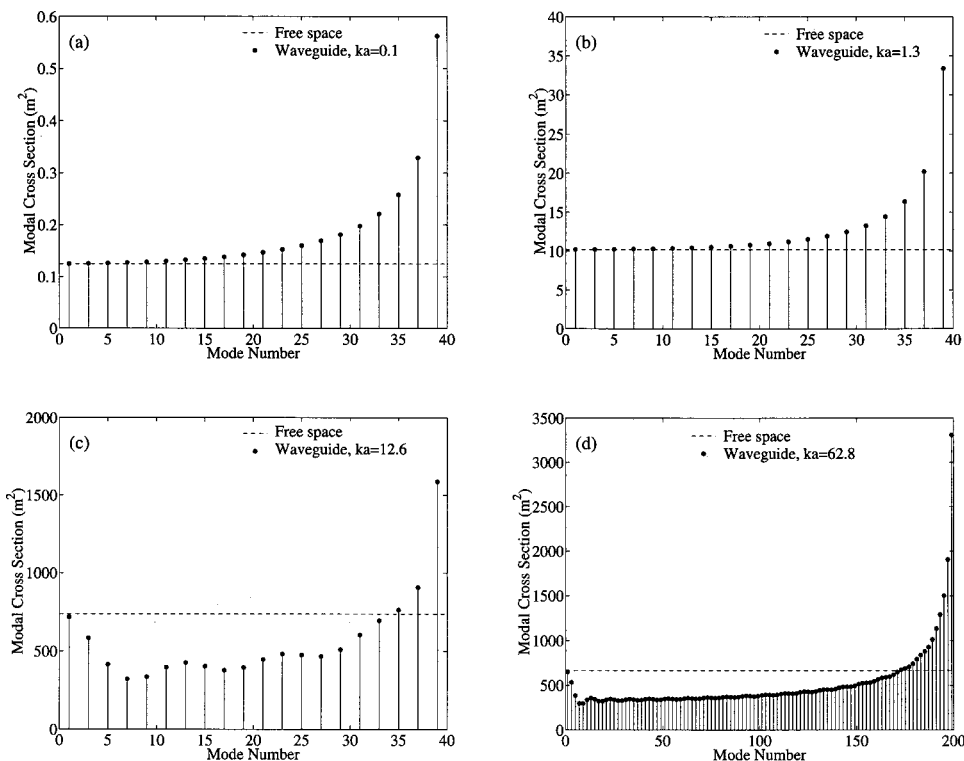


FIG. 14. Modal cross section Eq. (20) of a pressure release sphere at 50 m water depth for the extinction of the individual modes in a perfectly reflecting wave guide with (a) sphere radius 0.1 m, 300 Hz source frequency, $ka=0.1$, (b) sphere radius 1 m, 300 Hz source frequency, $ka=1.3$, (c) sphere radius 10 m, 300 Hz source frequency, $ka=12.6$, and (d) sphere radius 10 m, 1500 Hz source frequency, $ka=62.8$. The modal cross section of the sphere for mode 1 in each case is almost equal to its free space cross section.

point source by an object of arbitrary size and shape in a stratified medium has been developed from wave theory. In a wave guide, both the incident and scattered fields are composed of a superposition of plane waves or equivalently a superposition of modes. The total extinction is shown to be a linear sum of the extinction of each wave guide mode. Each modal extinction involves a sum over all incident modes scattered into the given mode and is expressed in terms of the objects's plane wave scatter function in the forward azi-

muth and equivalent modal plane wave amplitudes. In general, our results show that when we have multiple plane waves incident on an object, whether in a wave guide or in free space, extinction will be a function of not only the forward scatter amplitude for each incident plane wave but also the scatter function amplitudes coupling each incident plane wave to all other plane waves with distinct directions that comprise the incident field.

Our derivation greatly facilitates scattering calculations

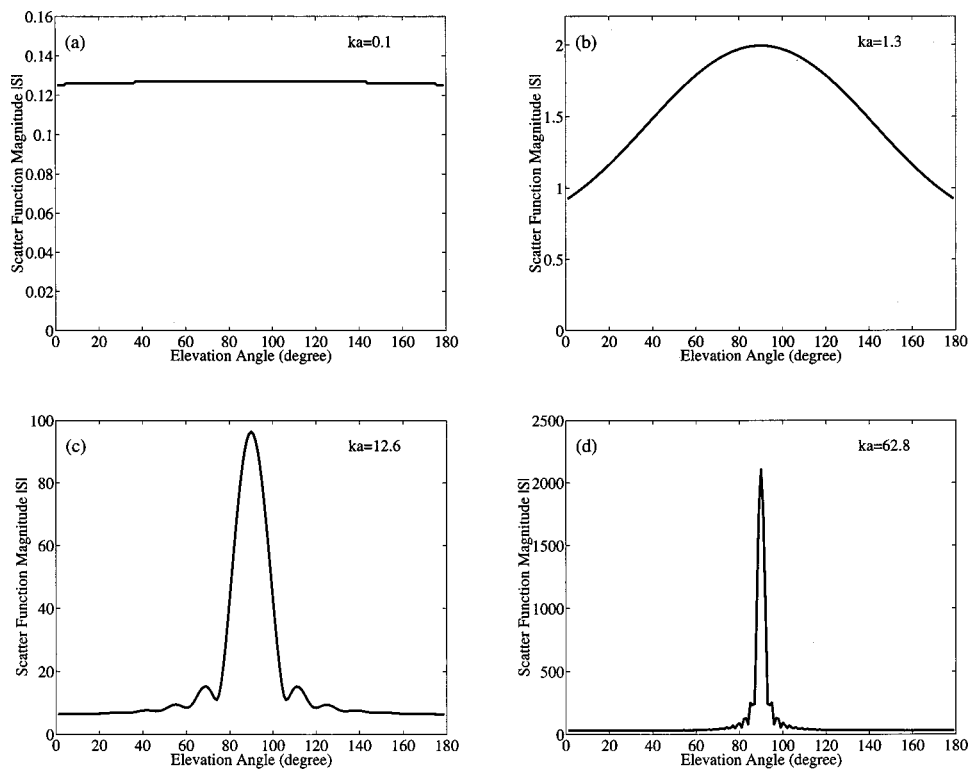


FIG. 15. The magnitude of the free space plane wave scatter function $S(\theta, \phi=0^\circ, \theta_i=90^\circ, \phi_i=0^\circ)$ is plotted as a function of θ , the elevation angle for a pressure release sphere at (a) $ka=0.1$, (b) $ka=1.3$, (c) $ka=12.6$, and (d) $ka=62.8$. The forward scatter peak is at $\theta=90^\circ$.

by eliminating the need to integrate energy flux about the object. The only assumptions are that multiple scattering between the object and wave guide boundaries is negligible, and the object lies within a constant sound speed layer.

Two extinction cross sections are defined for an object submerged in a wave guide. The first is the combined cross section which is the ratio of the combined extinction of all the modes of the wave guide to the total incident intensity in the radial direction at the object's centroid. Calculations for a shallow water wave guide show that both the combined extinction and the combined cross section of an object are highly dependent on measurement geometry, medium stratification, as well as the scattering properties of the object. They also fluctuate with range due to the coherent interference between the modes. Both are significantly modified by the presence of absorption in the medium. The presence of absorption typically means that the extinction and corresponding cross section of the obstacle in an ocean wave guide will be smaller than its value in free space. The practical implications of these findings is that experimental measurements of the total scattering cross section of an obstacle in a wave guide may differ greatly from those obtained for the same obstacle in free space and may lead to errors in target classification if the wave guide effects are not properly taken into account.

We also define the modal cross section of an object for the extinction of an individual wave guide mode of a wave guide. We show that for an object submerged in a typical ocean wave guide, the modal cross section for the extinction of mode 1 is almost identical to the object's free space cross section, after correcting for absorption loss in the medium. This finding can be used to robustly estimate the size of objects submerged underwater from extinction measurements involving mode 1, which is often the dominant mode after long range propagation in a shallow water wave guide.

APPENDIX A: GENERAL APPROACH FOR CALCULATING EXTINCTION

There are two approaches to calculate the extinction of an incident field due to absorption and scattering by an object. In the first approach, we define a closed control surface C that encloses the object, but excludes the source. We let the origin of the coordinate system be at the object centroid. Let \mathbf{r}_0 be the position of the source and \mathbf{r} be the position of a point on the control surface.

In the absence of the object, only the incident field Φ_i exists. The intensity of the incident field at location \mathbf{r} on the control surface from a source at \mathbf{r}_0 is

$$\mathbf{I}_i(\mathbf{r}|\mathbf{r}_0) = \Re\{\mathbf{V}_i^*(\mathbf{r}|\mathbf{r}_0)\Phi_i(\mathbf{r}|\mathbf{r}_0)\}, \quad (\text{A1})$$

where $\mathbf{V}_i(\mathbf{r}|\mathbf{r}_0)$ is the velocity vector of the incident field which, from Newton's law, can be expressed as

$$\mathbf{V}_i(\mathbf{r}|\mathbf{r}_0) = \frac{1}{i\omega d(\mathbf{r})} \nabla \Phi_i(\mathbf{r}|\mathbf{r}_0) \quad (\text{A2})$$

for a harmonic field at frequency ω where $d(\mathbf{r})$ is the density at location \mathbf{r} . Integrating the incident intensity over the entire

control surface C gives the net incident intensity flux \mathcal{F}_i through the control surface,

$$\mathcal{F}_i = \Re\left\{ \oint_C \mathbf{V}_i^* \Phi_i \cdot \mathbf{dS} \right\}. \quad (\text{A3})$$

In a lossless media, the incident energy flux entering the control surface has to equal that leaving the surface. Therefore in a lossless media,

$$\mathcal{F}_i = 0. \quad (\text{A4})$$

In the presence of the object, the total field at location \mathbf{r} on the control surface for a source at \mathbf{r}_0 is the sum of the incident pressure field from the source and the scattered field from the object,

$$\Phi_T(\mathbf{r}|\mathbf{r}_0) = \Phi_i(\mathbf{r}|\mathbf{r}_0) + \Phi_s(\mathbf{r}|\mathbf{r}_0). \quad (\text{A5})$$

The intensity of this total field at \mathbf{r} on the control surface is

$$\mathbf{I}_T(\mathbf{r}|\mathbf{r}_0) = \Re\{\mathbf{V}_T^*(\mathbf{r}|\mathbf{r}_0)\Phi_T(\mathbf{r}|\mathbf{r}_0)\}. \quad (\text{A6})$$

The total intensity integrated over the entire control surface C is the total energy flux \mathcal{F}_T through C , or the total intercepted power,

$$\begin{aligned} \mathcal{F}_T &= \Re\left\{ \oint_C \mathbf{V}_T^* \Phi_T \cdot \mathbf{dS} \right\} \\ &= \Re\left\{ \oint_C (\mathbf{V}_i^* \Phi_i + \mathbf{V}_i^* \Phi_s + \mathbf{V}_s^* \Phi_i + \mathbf{V}_s^* \Phi_s) \cdot \mathbf{dS} \right\}. \end{aligned} \quad (\text{A7})$$

If the object absorbs some of the power incident on it, the net outward power flow through the control surface is equal in magnitude to the rate at which absorption takes place. Let W_a be the rate at which energy is absorbed by the obstacle, then $\mathcal{F}_T = -W_a$.

Let W_s be the total power scattered in all directions by the object,

$$W_s = \Re\left\{ \oint_C \mathbf{V}_s^* \Phi_s \cdot \mathbf{dS} \right\}. \quad (\text{A8})$$

By definition, extinction is the sum of the total power absorbed and scattered by the object. Making use of Eqs. (A3), (A4), and (A8) in Eq. (A7), the extinction \mathcal{E} due to the object in a lossless media is

$$\mathcal{E} = W_a + W_s = -\Re\left\{ \oint_C (\mathbf{V}_i^* \Phi_s + \mathbf{V}_s^* \Phi_i) \cdot \mathbf{dS} \right\}. \quad (\text{A9})$$

From Eq. (A9) we see that extinction is a result of the interference between the incident and scattered fields over the control surface. For a plane wave in free space, the active region of the control surface over which the incident and scattered fields have a fixed phase relationship to interfere destructively lies within an angular width $\sqrt{\lambda}/r$ of the forward direction, where λ is the wavelength of the incident wave, and r is the distance of the control surface from the object centroid in the forward direction.^{2,3,17} This region comprises the shadow remnant. Outside of this region, the

integrand in Eq. (A9) fluctuates too rapidly to contribute to the extinction.

Consequently, instead of integrating the interference flux over the entire control surface, we can replace the enclosed control surface by a screen S_c in the forward direction. From Eq. (A7), if we integrate the interference flux over the area of the screen, instead of the enclosed control volume, we obtain

$$-\Re\left\{\int\int_{S_c}(\mathbf{V}_i^*\Phi_s+\mathbf{V}_s^*\Phi_i)\cdot d\mathbf{S}\right\} \\ =\Re\left\{\int\int_{S_c}(\mathbf{V}_i^*\Phi_i-\mathbf{V}_T^*\Phi_T+\mathbf{V}_s^*\Phi_s)\cdot d\mathbf{S}\right\}. \quad (\text{A10})$$

The first term on the right-hand side of Eq. (A10) is the incident flux \mathcal{F}_i through the screen, which is the flux through the screen in the absence of the object. The second term is \mathcal{F}_T , the total flux through the screen in the presence of the object. The last term is the scattered flux through the screen. If we place the screen sufficiently far from the object so that \mathbf{V}_s^* and Φ_s become small relative to \mathbf{V}_i^* and Φ_i due to spreading loss, the scattered flux becomes negligible. For instance, for plane waves in free space, the spherical spreading of the scattered field causes the scattered field intensity to decrease with range with a $1/r^2$ dependence, while the incident intensity remains constant.

At any given range r of the screen from the object, to measure the full extinction caused by the object, the screen has to be much wider than $\sqrt{\lambda r}$. For a sufficiently large screen, the extinction \mathcal{E} is, from Eq. (A10),

$$\mathcal{E}=\mathcal{F}_i-\mathcal{F}_T=-\Re\left\{\int\int_{S_c}(\mathbf{V}_i^*\Phi_s+\mathbf{V}_s^*\Phi_i)\cdot d\mathbf{S}\right\}, \quad (\text{A11})$$

the difference between the incident flux measured by the screen in the absence of the object and the total flux in the presence of the object. This is the approach due to Van de Hulst for calculating the extinction by placing a sufficiently large screen in the forward direction to register the full extinction.

APPENDIX B: EXTINCTION, ABSORPTION, AND SCATTERING CROSS SECTIONS

The extinction, absorption, and scattering cross sections can be viewed as fictitious areas that intercept a portion of the incident power equal to the extinguished, absorbed or scattered power, respectively. The extinction cross section σ_T , by definition, is the ratio between the rate of dissipation of energy \mathcal{E} and the rate at which energy is incident on unit cross-sectional area of the object I_i ,

$$\sigma_T=\frac{\mathcal{E}}{I_i}. \quad (\text{B1})$$

From Eq. (A9), we can also express the above as

$$\sigma_T=\frac{W_a+W_s}{I_i}=\sigma_a+\sigma_s, \quad (\text{B2})$$

where σ_a and σ_s are the absorption and scattering cross sections, respectively. For a nonabsorbing object, $\sigma_a=0$, and

the extinction cross section is then equal to the scattering cross section, $\sigma_T=\sigma_s$.

APPENDIX C: EXTINCTION FORMULA FOR SCATTERING IN AN INFINITE LOSSY UNBOUNDED MEDIA

We derive the formula for the extinction of an incident plane wave in the far field of a point source by an object in an infinite unbounded medium with absorption loss. We will derive the expression using both the control surface method and the Hulst screen method discussed in Appendix A and compare the resulting expressions. Let ν be the coefficient for absorption in the medium. We write the magnitude of the complex wave vector as $k=\kappa+i\nu$, where $\kappa=\omega/c$.

The object centroid coincides with the center of the coordinate system and we place the source at $\mathbf{r}_0=(0,0,-z_0)$. First we derive the formula using the control surface method, Eq. (A9). We let the control surface be a spherical surface of radius R centered at the object centroid. At any point \mathbf{r} on the control surface, the incident field is given by the free space Green's function,

$$\Phi_i(\mathbf{r}|\mathbf{r}_0)=\frac{1}{4\pi}\frac{e^{ik|\mathbf{r}-\mathbf{r}_0|}}{|\mathbf{r}-\mathbf{r}_0|}. \quad (\text{C1})$$

Since the object is in the far field of the point source, the incident field at the object can be approximated as composing of plane waves with amplitude $e^{ikz_0}/4\pi z_0$. The scattered field from the object at ranges far from the object can be expressed as

$$\Phi_s(\mathbf{r}|\mathbf{r}_0)=\frac{1}{4\pi}\frac{e^{ikz_0}}{z_0}\frac{e^{ikr}}{kr}S(\theta,\phi;0,0). \quad (\text{C2})$$

The first term in the integrand of Eq. (A9) for this case is

$$\mathbf{V}_i^*\Phi_s=\frac{1}{16\pi^2}\frac{(\kappa-i\nu)}{\omega d}\frac{e^{-i\kappa\sqrt{x^2+y^2+(z+z_0)^2}}}{(x^2+y^2+(z+z_0)^2)}(r\mathbf{i}_r+z_0\mathbf{i}_z) \\ \times\frac{e^{ikz_0}}{z_0}\frac{e^{i\kappa\sqrt{x^2+y^2+z^2}}}{(\kappa+i\nu)\sqrt{x^2+y^2+z^2}}S(\theta,\phi;0,0) \\ \times e^{-\nu\sqrt{x^2+y^2+(z+z_0)^2}}e^{-\nu z_0}e^{-\nu\sqrt{x^2+y^2+z^2}}. \quad (\text{C3})$$

In the above expression, we explicitly factor out the term representing absorption in the medium to avoid confusion when conjugating the fields and to keep track of absorption losses in the medium. On the control surface, $r=\sqrt{x^2+y^2+z^2}=R$. We will assume that $z_0\gg R$ since the object is in the far field of the point source. We use the approximation $\sqrt{x^2+y^2+(z+z_0)^2}\approx z+z_0$ in the term that determines the phase of the integrand, and the approximation $\sqrt{x^2+y^2+(z+z_0)^2}\approx z_0$ in the spreading loss factor. The resulting expression becomes,

$$\mathbf{V}_i^*\Phi_s=\frac{1}{16\pi^2}\frac{(\kappa-i\nu)}{\omega d(\kappa+i\nu)}\frac{e^{-i(\kappa+\nu)z}}{z_0^3}(z_0\mathbf{i}_z+R\mathbf{i}_r)\frac{e^{i\kappa R}}{R} \\ \times S(\theta,\phi;0,0)e^{-2\nu z_0}e^{-\nu R}. \quad (\text{C4})$$

Next, we integrate Eq. (C4) over the area of the enclosed spherical surface. An area element on the surface is

$\mathbf{dS} = \mathbf{i}_r R^2 \sin \theta d\theta d\phi$. Since $z_0 \gg R$ we need only consider the first term in Eq. (C4) and note that $\mathbf{i}_z \cdot \mathbf{i}_r = \cos \theta$. With $z = R \cos \theta$ on the spherical surface, we obtain

$$\begin{aligned} \oint_C \oint_C \mathbf{V}_i^* \Phi_s \cdot \mathbf{dS} &= \frac{1}{16\pi^2} \frac{(\kappa - i\nu)}{\omega d (\kappa + i\nu) z_0^2 R} e^{i\kappa R} \\ &\times e^{-2\nu z_0} e^{-\nu R} \\ &\times \int_0^\pi \int_0^{2\pi} e^{-(i\kappa + \nu)R \cos(\theta)} S(\theta, \phi; 0, 0) \\ &\times \cos \theta \sin \theta d\theta d\phi. \end{aligned} \quad (\text{C5})$$

Making use of asymptotic integration,

$$\begin{aligned} \oint_C \oint_C \mathbf{V}_i^* \Phi_s \cdot \mathbf{dS} &= \frac{i}{8\pi\omega d z_0^2} \frac{1}{\kappa + i\nu} e^{-2\nu z_0} (S(0, 0; 0, 0) e^{-2\nu R} \\ &+ S(0, \pi; 0, 0) e^{i2\kappa R}). \end{aligned} \quad (\text{C6})$$

Similarly, we integrate the second term of Eq. (A9) over the control surface and obtain

$$\begin{aligned} \oint_C \oint_C \mathbf{V}_s^* \Phi_i \cdot \mathbf{dS} &= \frac{-i}{8\pi\omega d z_0^2} \frac{1}{\kappa + i\nu} e^{-2\nu z_0} (S^*(0, 0; 0, 0) e^{-2\nu R} \\ &- S^*(0, \pi; 0, 0) e^{-i2\kappa R}). \end{aligned} \quad (\text{C7})$$

Summing Eqs. (C6) and (C7), taking only the negative of the real part of the sum, we obtain the extinction caused by an object in an infinite unbounded lossy medium using the control volume method,

$$\begin{aligned} \mathcal{E}_C(\mathbf{r}|\mathbf{r}_0) &= \frac{1}{4\pi\omega d} \frac{e^{-2\nu(z_0+R)}}{z_0^2} \left(\frac{\kappa}{\kappa^2 + \nu^2} \Im\{S(0, 0; 0, 0)\} \right. \\ &\left. - \frac{\nu}{\kappa^2 + \nu^2} \Re\{S(0, \pi; 0, 0) e^{i2\kappa R}\} e^{2\nu R} \right). \end{aligned} \quad (\text{C8})$$

Next, we derive the extinction using the Van de Hulst screen method, Eq. (A11). We start with the expression in Eq. (C3). We place a square screen of length L a sufficiently large distance from the object in the forward direction, parallel to the $x-y$ plane a distance z away from the object. As discussed in Appendix A, we require $L > \sqrt{\lambda}z$. Since z is large, we assume that for points on the active region of the screen, $z \gg \rho$ where $\rho = \sqrt{x^2 + y^2}$. We use the approximations $\sqrt{x^2 + y^2 + (z+z_0)^2} \approx z + z_0 + [\rho^2/2(z+z_0)]$, and $\sqrt{x^2 + y^2 + z^2} \approx z + (\rho^2/2z)$ in the terms that determine the phase of the integrand, and the approximations $\sqrt{x^2 + y^2 + (z+z_0)^2} \approx z + z_0$ and $\sqrt{x^2 + y^2 + z^2} \approx z$ in the absorption and spreading loss factors. Equation (C3) simplifies to

$$\begin{aligned} \mathbf{V}_i^* \Phi_s &= \frac{1}{16\pi^2} \frac{(\kappa - i\nu)}{(\kappa + i\nu)} \frac{1}{\omega d z_0 z (z_0 + z)} \\ &\times e^{i\kappa z_0 \rho^2/2z(z_0+z)} S(\theta, \phi; 0, 0) e^{-2\nu(z_0+z)}. \end{aligned} \quad (\text{C9})$$

We integrate Eq. (C9) using Eq. (A11) over the area of the screen. With the screen lying normal to the z axis, an area element of the screen is $\mathbf{dS} = \mathbf{i}_z dx dy$,

$$\begin{aligned} \int \int_{S_c} \mathbf{V}_i^* \Phi_s \cdot \mathbf{dS} &= \frac{1}{16\pi^2} \frac{(\kappa - i\nu)}{(\kappa + i\nu)} \frac{1}{\omega d z_0 z (z_0 + z)} e^{-2\nu(z_0+z)} \\ &\times \int_{-L/2}^{L/2} \int_{-L/2}^{L/2} e^{i\kappa z_0 \rho^2/2z(z_0+z)} S(\theta, \phi; 0, 0) dx dy. \end{aligned} \quad (\text{C10})$$

As discussed in Appendix A, the angular width of the active area on the screen is of the order of $\sqrt{\lambda}/z$ which is small for large z . We therefore approximate the scatter function with its value at $\theta = \phi = 0$ and factor it out of the integral above. Integrating the resulting expression using asymptotic integration, we obtain

$$\begin{aligned} \int \int_{S_c} \mathbf{V}_i^* \Phi_s \cdot \mathbf{dS} &= \frac{i}{8\pi\omega d z_0^2} \frac{1}{\kappa} S(0, 0; 0, 0) \frac{(\kappa - i\nu)}{(\kappa + i\nu)} e^{-2\nu(z_0+z)}. \end{aligned} \quad (\text{C11})$$

Similarly, we integrate the second term in Eq. (A11) to obtain

$$\int \int_{S_c} \mathbf{V}_s^* \Phi_i \cdot \mathbf{dS} = \frac{-i}{8\pi\omega d z_0^2} \frac{1}{\kappa} S^*(0, 0; 0, 0) e^{-2\nu(z_0+z)}. \quad (\text{C12})$$

Adding the two expressions and taking only the negative of the real part of the sum, we obtain the extinction caused by an object in an infinite unbounded lossy medium using the screen method,

$$\begin{aligned} \mathcal{E}_{S_c}(\mathbf{r}|\mathbf{r}_0) &= \frac{1}{4\pi\omega d} \frac{e^{-2\nu(z+z_0)}}{z_0^2} \frac{1}{\kappa} \\ &\times \left(\Im\{S(0, 0; 0, 0)\} - \frac{\nu}{\kappa} \Re\{S(0, 0; 0, 0)\} \right). \end{aligned} \quad (\text{C13})$$

The expression for the extinction using the control volume method Eq. (C8) and that obtained using Van de Hulst screen method Eq. (C13) are equal if $\nu = 0$. The second term in both equations arise due to absorption by the medium. The expressions for the absorption loss term differ because we integrate the energy flux over different surfaces. If ν is small compared to κ , $\nu/\kappa \ll 1$, we can ignore the second term in both equations, and letting $z = R$, the resulting expressions for the extinction are identical and become

$$\mathcal{E}(\mathbf{r}|\mathbf{r}_0) = \frac{1}{4\pi\omega d \kappa} \Im\{S(0, 0; 0, 0)\} \frac{e^{-2\nu(z+z_0)}}{z_0^2}. \quad (\text{C14})$$

This derivation shows that the screen method gives the true

extinction only if the absorption loss in the medium is small. From Eq. (C14), we see that absorption in the medium lowers the extinction that we would otherwise measure in a lossless medium. The $1/z_0^2$ factor is due to the spherical spreading of the incident field from the source to the object.

The incident intensity on the object in the z direction for $\nu/\kappa \ll 1$ is

$$\mathbf{V}_i^* \Phi_i = \frac{1}{16\pi^2} \frac{\kappa}{\omega d} \frac{e^{-2\nu z_0}}{z_0^2}. \quad (\text{C15})$$

Dividing the extinction in Eq. (C14) with the incident intensity on the object Eq. (C15), we obtain the extinction cross section of the object in the infinite unbounded lossy media,

$$\sigma_T(z) = \frac{4\pi}{\kappa^2} \mathcal{I}\{S(0,0;0,0)\} e^{-2\nu z}. \quad (\text{C16})$$

Equation (C16) shows that a measurement of the cross section of an object in a lossy medium will be smaller than in a lossless medium. To obtain the true cross section of the object, independent of the medium, we have to correct for absorption in the lossy medium.

APPENDIX D: EXTINCTION FORMULA FOR SCATTERING IN A STRATIFIED WAVE GUIDE CALCULATED USING A CONTROL SURFACE THAT ENCLOSES THE OBJECT

Let the control surface be a semi-infinite cylinder of radius R with a cap at the sea surface where $z = -D$, similar to that defined in Sec. III. The axis of the cylinder is parallel to the z axis and passes through the object centroid. The source is located at $\mathbf{r}_0 = (-x_0, 0, z_0)$, and we assume that $R \ll x_0$.

As discussed in Sec. III, the sea has a pressure-release surface where both the incident and scattered fields vanish. The contribution of the interference flux through the cap at the sea surface $z = -D$ is zero. We need only integrate the interference flux in Eq. (A9) over the curved surface of the cylinder to obtain the extinction caused by the object.

Using Eqs. (1), (2), (3), and (A2), the first term in the integrand of Eq. (A9) on the curved surface of the cylinder, $\mathbf{R} = (x, y, z)$ is

$$\begin{aligned} \mathbf{V}_i^* \Phi_s = & \frac{i}{d(z)d(z_0)d(0)2\omega k} \sum_{l=1}^{\infty} \sum_{m=1}^{\infty} \sum_{n=1}^{\infty} u_l^*(z_0) u_m(z) \left[\frac{\partial}{\partial z} u_l^*(z) \mathbf{i}_z - i \xi_l^* u_l^*(z) \mathbf{i}_x \right] \frac{e^{-i\Re\{\xi_l\}(x_0+x)}}{\sqrt{\xi_l^* x_0}} \frac{e^{i\Re\{\xi_m\}R}}{\sqrt{\xi_m R}} \\ & \times [N_m^- e^{i\Re\{\gamma_m\}D} A_n(\mathbf{r}_0) S(\pi - \alpha_m, \phi; \alpha_n, 0) - N_m^+ e^{-i\Re\{\gamma_m\}D} A_n(\mathbf{r}_0) S(\alpha_m, \phi; \alpha_n, 0) \\ & - N_m^- e^{i\Re\{\gamma_m\}D} B_n(\mathbf{r}_0) S(\pi - \alpha_m, \phi; \pi - \alpha_n, 0) + N_m^+ e^{-i\Re\{\gamma_m\}D} B_n(\mathbf{r}_0) S(\alpha_m, \phi; \pi - \alpha_n, 0)] e^{-\Im\{\xi_l\}x_0} e^{-\Im\{\gamma_m\}D}. \quad (\text{D1}) \end{aligned}$$

In the above expression, the terms representing absorption by the wave guide have been factored out explicitly to avoid confusion when conjugating the fields and also to keep track of absorption losses due to the wave guide. Since $R \ll x_0$, the expansion $|\boldsymbol{\rho} - \boldsymbol{\rho}_0| = x_0 + x$ was used in the terms that determine the phase of the integrand while the approximation $|\boldsymbol{\rho} - \boldsymbol{\rho}_0| \approx x_0$ was used in the spreading and absorption loss factors. We ignore the absorption loss term $e^{-\Im\{\xi_l\}R}$ since it is small compared to $e^{-\Im\{\xi_l\}x_0}$.

Next we integrate Eq. (D1) over the curved surface of the cylinder. An area element on the surface of the cylinder is $d\mathbf{S} = \mathbf{i}_\rho R d\phi dz$. We use the orthogonality relation in Eq. (4) between the modes $u_l^*(z)$ and $u_m(z)$ to integrate Eq. (D1) over the semi-infinite depth of the cylinder in the wave guide. This reduces the triple sum over the modes to a double sum,

$$\begin{aligned} \oint_C \oint_C \mathbf{V}_i^* \Phi_s \cdot d\mathbf{S} = & \int_0^{2\pi} \int_{-D}^{\infty} \mathbf{V}_i^* \Phi_s \cdot \mathbf{i}_\rho R dz d\phi \\ = & \frac{1}{d(z_0)d(0)2\omega k} \sum_{m=1}^{\infty} \sum_{n=1}^{\infty} \frac{\xi_m^*}{|\xi_m| \sqrt{x_0 R}} u_m^*(z_0) e^{i\Re\{\xi_m\}R} e^{-i\Re\{\xi_m\}x_0} \\ & \times \left\{ \int_0^{2\pi} [N_m^- e^{i\Re\{\gamma_m\}D} A_n(\mathbf{r}_0) S(\pi - \alpha_m, \phi; \alpha_n, 0) - N_m^+ e^{-i\Re\{\gamma_m\}D} A_n(\mathbf{r}_0) S(\alpha_m, \phi; \alpha_n, 0) \right. \\ & - N_m^- e^{i\Re\{\gamma_m\}D} B_n(\mathbf{r}_0) S(\pi - \alpha_m, \phi; \pi - \alpha_n, 0) + N_m^+ e^{-i\Re\{\gamma_m\}D} B_n(\mathbf{r}_0) S(\alpha_m, \phi; \pi - \alpha_n, 0)] \\ & \left. \times e^{-i\Re\{\xi_m\}R} \cos \phi \cos \phi R d\phi \right\} e^{-\Im\{\xi_m\}x_0} e^{-\Im\{\gamma_m\}D}. \quad (\text{D2}) \end{aligned}$$

The integral involving ϕ can be evaluated using the method of stationary phase. There are two stationary phase points corresponding to the forward azimuth $\phi=0$, and the back azimuth $\phi=\pi$. Applying the result of the following stationary phase integration over the azimuth angle ϕ ,

$$\int_0^{2\pi} S(\pi - \alpha_m, \phi; \alpha_n, 0) e^{-i\Re\{\xi_m\}R \cos \phi} \cos \phi d\phi = \sqrt{\frac{2\pi}{\Re\{\xi_m\}R}} e^{i\pi/4} [e^{-i\Re\{\xi_m\}R} S(\pi - \alpha_m, 0; \alpha_n, 0) + i e^{i\Re\{\xi_m\}R} S(\pi - \alpha_m, \pi; \alpha_n, 0)], \quad (D3)$$

to Eq. (D2), the integration of the first term in Eq. (A9) over the curved surface of the cylinder in the wave guide becomes

$$\begin{aligned} \oint_C \oint_C \mathbf{V}_i^* \Phi_s \cdot d\mathbf{S} &= \frac{1}{d^2(z_0)d(0)4\omega k} \frac{1}{x_0} \sum_{m=1}^{\infty} \sum_{n=1}^{\infty} \frac{\xi_m^*}{|\xi_m| \sqrt{\Re\{\xi_m\} \xi_n^*}} u_m^*(z_0) u_n(z_0) e^{i\Re\{\xi_n - \xi_m\}x_0} \\ &\times (i[N_m^- N_n^- e^{i\Re\{\gamma_m + \gamma_n\}D} S(\pi - \alpha_m, 0; \alpha_n, 0) - N_m^+ N_n^- e^{i\Re\{-\gamma_m + \gamma_n\}D} S(\alpha_m, 0; \alpha_n, 0) \\ &- N_m^- N_n^+ e^{i\Re\{\gamma_m - \gamma_n\}D} S(\pi - \alpha_m, 0; \pi - \alpha_n, 0) + N_m^+ N_n^+ e^{i\Re\{-\gamma_m - \gamma_n\}D} S(\alpha_m, 0; \pi - \alpha_n, 0)] \\ &- e^{i\Re\{2\xi_m\}R} [N_m^- N_n^- e^{i\Re\{\gamma_m + \gamma_n\}D} S(\pi - \alpha_m, \pi; \alpha_n, 0) - N_m^+ N_n^- e^{i\Re\{-\gamma_m + \gamma_n\}D} S(\alpha_m, \pi; \alpha_n, 0) \\ &- N_m^- N_n^+ e^{i\Re\{\gamma_m - \gamma_n\}D} S(\pi - \alpha_m, \pi; \pi - \alpha_n, 0) + N_m^+ N_n^+ e^{i\Re\{-\gamma_m - \gamma_n\}D} S(\alpha_m, \pi; \pi - \alpha_n, 0)]) \\ &\times e^{-i\Re\{\xi_m + \xi_n\}x_0} e^{-\Im\{\gamma_m + \gamma_n\}D}. \end{aligned} \quad (D4)$$

Similarly, we can evaluate the second term in Eq. (A9) which gives

$$\begin{aligned} \oint_C \oint_C \mathbf{V}_s^* \Phi_i \cdot d\mathbf{S} &= -\frac{1}{d^2(z_0)d(0)4\omega k} \frac{1}{x_0} \sum_{m=1}^{\infty} \sum_{n=1}^{\infty} \frac{\xi_m^*}{|\xi_m| \sqrt{\Re\{\xi_m\} \xi_n^*}} u_m(z_0) u_n^*(z_0) e^{-i\Re\{\xi_n - \xi_m\}x_0} \\ &\times (i[N_m^{*-} N_n^{*-} e^{-i\Re\{\gamma_m + \gamma_n\}D} S^*(\pi - \alpha_m, 0; \alpha_n, 0) - N_m^{*+} N_n^{*-} e^{-i\Re\{-\gamma_m + \gamma_n\}D} S^*(\alpha_m, 0; \alpha_n, 0) \\ &- N_m^{*-} N_n^{*+} e^{-i\Re\{\gamma_m - \gamma_n\}D} S^*(\pi - \alpha_m, 0; \pi - \alpha_n, 0) + N_m^{*+} N_n^{*+} e^{-i\Re\{-\gamma_m - \gamma_n\}D} S^*(\alpha_m, 0; \pi - \alpha_n, 0)] \\ &- e^{-i\Re\{2\xi_m\}R} [N_m^{*-} N_n^{*-} e^{-i\Re\{\gamma_m + \gamma_n\}D} S^*(\pi - \alpha_m, \pi; \alpha_n, 0) - N_m^{*+} N_n^{*-} e^{-i\Re\{-\gamma_m + \gamma_n\}D} S^*(\alpha_m, \pi; \alpha_n, 0) \\ &- N_m^{*-} N_n^{*+} e^{-i\Re\{\gamma_m - \gamma_n\}D} S^*(\pi - \alpha_m, \pi; \pi - \alpha_n, 0) + N_m^{*+} N_n^{*+} e^{-i\Re\{-\gamma_m - \gamma_n\}D} S^*(\alpha_m, \pi; \pi - \alpha_n, 0)]) \\ &\times e^{-\Re\{\xi_m + \xi_n\}x_0} e^{-\Im\{\gamma_m + \gamma_n\}D}. \end{aligned} \quad (D5)$$

We then sum Eqs. (D4) and (D5), taking only the negative of the real part of the sum following Eq. (A9). This leads to the range dependent extinction $\mathcal{E}(R|\mathbf{r}_0)$ of the incident field in a wave guide due to an object at the origin measured by a cylinder of radius R centered on the object with source at \mathbf{r}_0 ,

$$\begin{aligned} \mathcal{E}(R|\mathbf{r}_0) &= \frac{1}{d^2(z_0)d(0)2\omega k} \frac{1}{x_0} \sum_{m=1}^{\infty} \sum_{n=1}^{\infty} \frac{\sqrt{\Re\{\xi_m\}}}{|\xi_m|} \Im \left\{ \frac{1}{\sqrt{\xi_n}} u_m^*(z_0) u_n(z_0) e^{i\Re\{\xi_n - \xi_m\}x_0} \right. \\ &\times [N_m^- N_n^- e^{i\Re\{\gamma_m + \gamma_n\}D} S(\pi - \alpha_m, 0; \alpha_n, 0) - N_m^+ N_n^- e^{i\Re\{-\gamma_m + \gamma_n\}D} S(\alpha_m, 0; \alpha_n, 0) \\ &- N_m^- N_n^+ e^{i\Re\{\gamma_m - \gamma_n\}D} S(\pi - \alpha_m, 0; \pi - \alpha_n, 0) + N_m^+ N_n^+ e^{i\Re\{-\gamma_m - \gamma_n\}D} S(\alpha_m, 0; \pi - \alpha_n, 0)] \left. \right\} e^{-\Re\{\xi_m + \xi_n\}x_0} e^{-\Im\{\gamma_m + \gamma_n\}D} \\ &+ \frac{1}{d^2(z_0)d(0)2\omega k} \frac{1}{x_0} \sum_{m=1}^{\infty} \sum_{n=1}^{\infty} \frac{\Im\{\xi_m\}}{|\xi_m| \sqrt{\Re\{\xi_m\}}} \Im \left\{ \frac{1}{\sqrt{\xi_n}} u_m^*(z_0) u_n(z_0) e^{i\Re\{\xi_n - \xi_m\}x_0} e^{i\Re\{2\xi_m\}R} \right. \\ &\times [N_m^- N_n^- e^{i\Re\{\gamma_m + \gamma_n\}D} S(\pi - \alpha_m, \pi; \alpha_n, 0) - N_m^+ N_n^- e^{i\Re\{-\gamma_m + \gamma_n\}D} S(\alpha_m, \pi; \alpha_n, 0) \\ &- N_m^- N_n^+ e^{i\Re\{\gamma_m - \gamma_n\}D} S(\pi - \alpha_m, \pi; \pi - \alpha_n, 0) + N_m^+ N_n^+ e^{i\Re\{-\gamma_m - \gamma_n\}D} S(\alpha_m, \pi; \pi - \alpha_n, 0)] \left. \right\} e^{-\Re\{\xi_m + \xi_n\}x_0} e^{-\Im\{\gamma_m + \gamma_n\}D}. \end{aligned} \quad (D6)$$

After comparing the expression for the extinction calculated using the control surface method Eq. (D6), with that obtained using the Van de Hulst screen method Eq. (13), we see that they are identical only in the perfectly reflecting waveguide where $\Im\{\xi_m\} = 0$. If the absorption loss in the waveguide is small, we can neglect the second term in Eq. (D6) and the resulting

expression will be similar to Eq. (13). The differences in Eqs. (13) and (D6) arise because of absorption loss in the medium and also because we integrate the energy fluxes over different surfaces in the two methods.

The Van de Hulst screen method is of more practical use because it represents the type of measurement that can be made with a standard 2D planar or billboard array. A control volume measurement, on the other hand, would be very difficult to implement since it would require an array that completely encloses the object.

¹M. Born and E. Wolf, *Principles of Optics, Electromagnetic Theory of Propagation Interference and Diffraction of Light*, 6th ed. (Cambridge University Press, Cambridge, 1980).

²H. C. van de Hulst, "On the attenuation of plane waves by obstacles of arbitrary size and form," *Physica (Amsterdam)* **15**, 740–746 (1949).

³L. I. Schiff, "On an expression for the total cross-section," *Prog. Theor. Phys.* **11**, 288–290 (1954).

⁴H. C. van de Hulst, *Light Scattering by Small Particles* (Dover, New York, 1981).

⁵R. J. Urick, *Principles of Underwater Sound* (McGraw-Hill, New York, 1983).

⁶P. M. Morse, *Theoretical Acoustics* (Princeton University Press, Princeton, NJ, 1986).

⁷B. V. Smith and M. G. Ertugrul, "A technique for the measurement of extinction cross-section," *J. Sound Vib.* **98**, 275–288 (1985).

⁸T. K. Stanton, "Multiple scattering with applications to fish-echo processing," *J. Acoust. Soc. Am.* **73**, 1164–1169 (1983).

⁹F. P. Mechel, "Iterative solutions for finite-size absorbers," *J. Sound Vib.* **134**, 489–506 (1989).

¹⁰Y. P. Guo, "On sound energy scattered by a rigid body near a compliant surface," *Proc. R. Soc. London* **1943**, 543–552 (1995).

¹¹F. Ingenito, "Scattering from an object in a stratified medium," *J. Acoust. Soc. Am.* **82**, 2051–2059 (1987).

¹²N. C. Makris and P. Ratilal, "A unified model for reverberation and submerged object scattering in a stratified ocean waveguide," *J. Acoust. Soc. Am.* **109**, 909–941 (2001).

¹³N. C. Makris, "A spectral approach to 3-D object scattering in layered media applied to scattering from submerged spheres," *J. Acoust. Soc. Am.* **104**, 2105–2113 (1998); **106**, 518(E) (1999).

¹⁴F. B. Jensen, W. A. Kuperman, M. B. Porter, and H. Schmidt, *Computational Ocean Acoustics* (American Institute of Physics, New York, 1994).

¹⁵G. V. Frisk, *Ocean and Seabed Acoustics, A Theory of Wave Propagation* (Prentice Hall, New Jersey, 1994).

¹⁶*Electromagnetic and Acoustic Scattering by Simple Shapes*, edited by J. J. Bowman, T. B. A. Senior, and P. L. E. Uslenghi (North-Holland, Amsterdam, 1969).

¹⁷N. C. Makris, F. Ingenito, and W. A. Kuperman, "Detection of a submerged object insonified by surface noise in an ocean waveguide," *J. Acoust. Soc. Am.* **96**, 1703–1724 (1994).